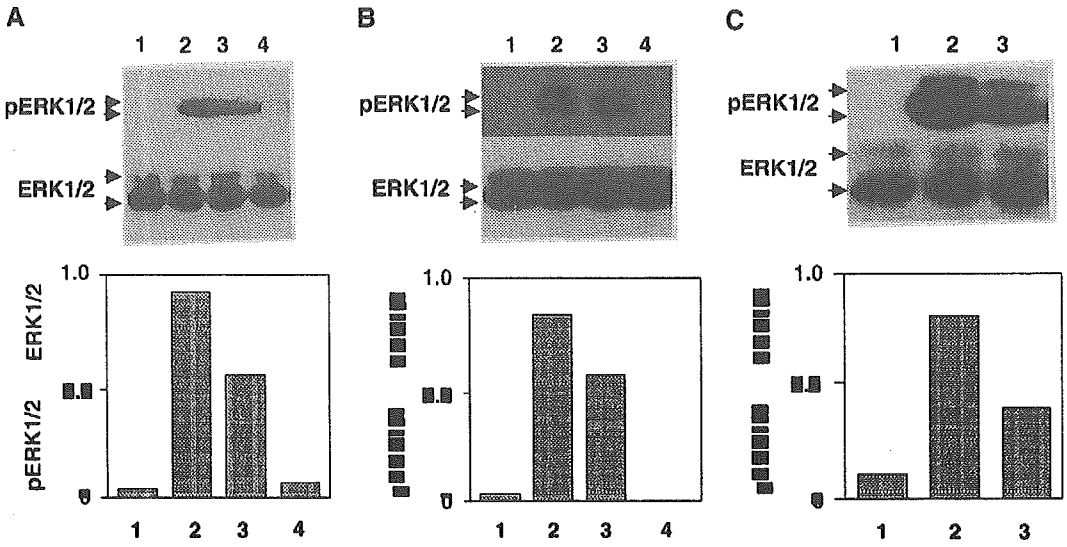

Fig. 3. Attenuation by CNP of MAPK activity of FGFs. CNP and cGMP reduced FGF-stimulated elevation of phosphorylated ERK1/2. ATDC5 cell extracts were examined with Western blotting for phosphorylated ERK1/2 (pERK1/2) and total ERK1/2 (ERK1/2) as described under Materials and methods. (A) CNP diminished FGF2-stimulated elevation of phosphorylated ERK1/2. 1: Vehicle, 2, 3, 4: stimulation with 10 ng/ml FGF2, 3: preincubation with 10^{-7} M CNP, 4: preincubation with 10^{-6} M CNP. (B) CNP attenuated FGF18-stimulated elevation of phosphorylated ERK1/2. 1: Vehicle, 2, 3, 4: stimulation with 10 ng/ml FGF18, 3: preincubation with 10^{-7} M CNP, 4: preincubation with 10^{-6} M CNP. (C) 8-bromo cGMP decreased FGF2-stimulated elevation of phosphorylated ERK1/2. 1: Vehicle, 2, 3: stimulation with 10 ng/ml FGF2, 3: preincubation with 10^{-4} M 8-Bromo cGMP. Representative blots are shown, and the relative levels of proteins were measured as phospho-ERK1/2/ERK1/2 density values. Each experiment was repeated 3 times, and data from a representative experiment are shown.

No change in STAT-1 phosphorylation in ATDC5 cells by FGFs or CNP

STAT-1 phosphorylation was already detectable at the basal level in ATDC5 cells. The level of phosphorylated STAT-1 remained unchanged when treated with FGF2 or FGF18 for 3, 10, 15, 30, or 60 min. Treatment of quiescent ATDC5 cells with CNP (10^{-7}–10^{-6} M) prior to the addition of FGF2 (10 ng/ml) and FGF18 (10 ng/ml) did not alter the amount of phosphorylated STAT-1 (Figs. 4A,

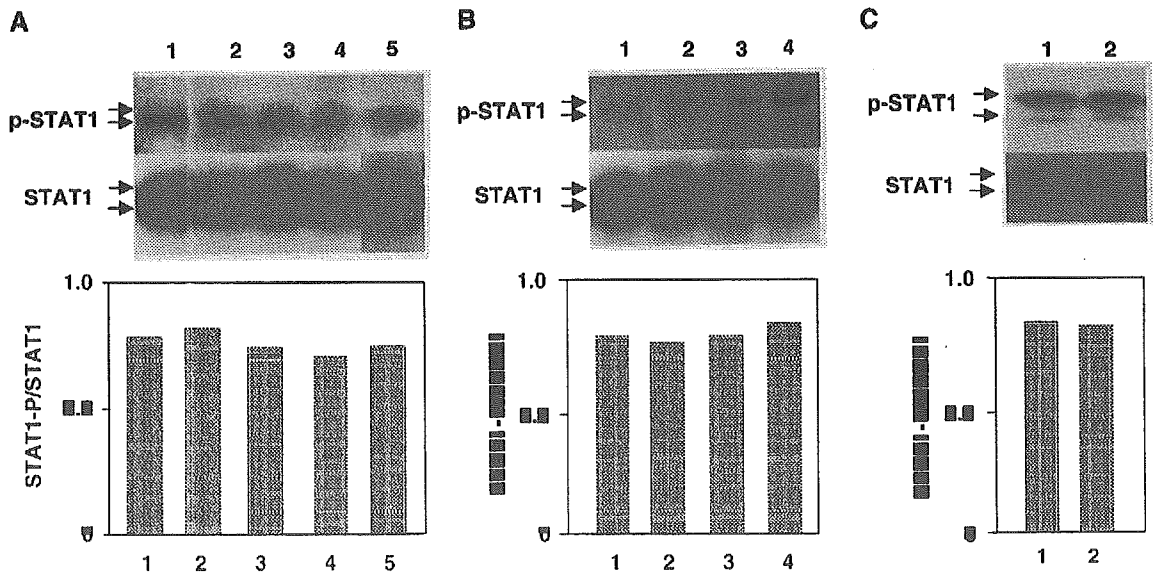

Fig. 4. No change in STAT-1 phosphorylation in ATDC5 cells by FGFs or CNP. Effects of CNP on the STAT-1 pathways of FGFs. ATDC5 cell extracts were examined with Western blotting for phosphorylated STAT-1 (pSTAT-1) and total STAT-1 (STAT-1) as described under Materials and methods. (A) CNP and 8-bromo cGMP did not alter the level of phosphorylated STAT-1 after FGF2 stimulation. 1: Vehicle, 2, 3, 4, 5: stimulation with 10 ng/ml FGF2, 3: preincubation with 10^{-7} M CNP, 4: preincubation with 10^{-6} M CNP, 5: preincubation with 10^{-4} M 8-bromo cGMP. (B) CNP did not alter the level of phosphorylated STAT-1 after FGF18 stimulation. 1: Vehicle, 2 3, 4: stimulation with 10 ng/ml FGF18, 3: preincubation with 10^{-7} M CNP, 4: preincubation with 10^{-6} M CNP. (C) CNP did not alter the basal expression of phosphorylated STAT-1. 1: Vehicle, 2: 10^{-6} M CNP alone. Representative blots are shown, and the relative levels of proteins were measured as the phospho-STAT-1/STAT-1 density values. Each experiment was repeated 3 times, and the data from a representative experiment are shown.

B), nor did CNP itself (10^{-6} M) affect the basal level of phosphorylated STAT-1 in ATDC5 cells (Fig. 4C), or treatment of quiescent ATDC5 cells with 10^{-4} M 8-bromo cGMP prior to the addition of FGF2 (10 ng/ml) cause no change in the amount of phosphorylated STAT-1 (Fig. 4A).

No effect of CNP on FGFR-3 expression in ATDC5 cells

FGFR3 mRNA levels in ATDC5 cells treated with the vehicle and pretreated with CNP (10^{-6} M) were 1.00 ± 0.06 and 1.04 ± 0.12 in arbitrary units, respectively, and this difference was not significant.

Effect of CNP and FGF18 on mouse fetal tibia organ culture

The organ culture of fetal mouse tibias provides a unique in vitro experimental model system of endochondral ossification. For our study, we used cultured tibias prepared from ICR mice, to examine the effects of CNP and FGF18. Treatment with 10^{-7} M CNP for 5 days produced a 12% increase in the total length of tibial explants compared with vehicle-treated explants (vehicle treated: 3.56 ± 0.05 mm vs. CNP treated: 3.99 ± 0.07 mm). On the other hand, treatment with 10 ng/ml FGF18 for 5 days resulted in a 6% decrease in the total length of tibial explants compared with vehicle-treated explants (vehicle treated: 3.57 ± 0.03 mm vs. FGF18 treated: 3.37 ± 0.04 mm). Treatment with a combination of 10^{-7} M CNP and 10 ng/ml FGF18 increased the total length of tibial explants for 8% compared with vehicle-treated explants (vehicle treated: 3.55 ± 0.04 mm vs. CNP and FGF18 treated: 3.84 ± 0.06 mm). These differences were all statistically significant ($P < 0.01$) (Fig. 5).

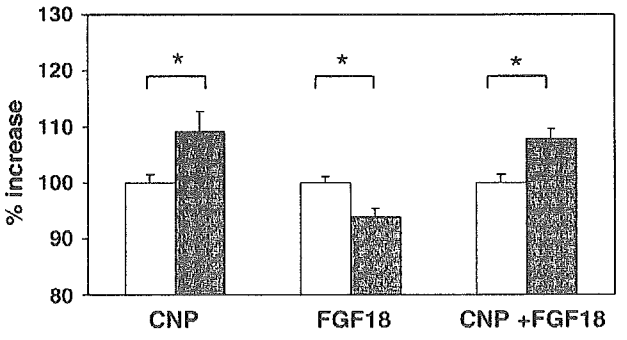

Fig. 5. Effect of CNP and FGF18 on mouse fetal tibia organ culture. Percent change in total length of fetal mouse tibias cultured with CNP and/or FGF18 for 5 days. Open columns show the percent change in total length of one tibia from mouse fetus treated with the vehicle. Hatched columns show the percent change in total length of the other tibia from the same mouse treated with 10^{-7} M CNP, 10 ng/ml FGF18, or with a combination of 10^{-7} M CNP and 10 ng/ml FGF18. Columns represent means ± SE ($n = 5$, each), *$P < 0.01$ vs. vehicle.

Effect of CNP and FGF18 on cell size and cell numbers of the growth plate chondrocytes

Microscopic examination disclosed elongation of the growth plate in mouse tibias cultured with 10^{-7} M CNP. Higher magnification of Alcian blue HE staining (Figs. 6A, B, E, F) and immunohistochemical staining for type X collagen (Figs. 6I, J) showed that the hypertrophic chondrocyte layer increased after treatment with 10^{-7} M CNP compared with treatment with the vehicle. The mean size of hypertrophic chondrocytes was markedly increased (vehicle treated: 497.85 ± 19.2 vs. CNP treated: 1071.42 ± 53.5 μm^2) (Fig. 7A), and the number of cells in the hypertrophic chondrocyte layer was reduced (vehicle treated: 152.67 ± 4.1 vs. CNP treated: 118 ± 3.61 cells) (Fig. 7B). In contrast, culturing with 10 ng/ml FGF18 caused shortening of the growth plate in cultured mouse tibias compared with that in vehicle-treated ones. Higher magnification of Alcian blue HE staining (Figs. 6A, C, E, G) and immunohistochemical staining for type X collagen (Figs. 6I, K) demonstrated that the hypertrophic chondrocyte layer was reduced. Not only the cell size (vehicle treated: 497.85 ± 19.2 vs. FGF18 treated: 314.01 ± 23.67 μm^2) (Fig. 7A), but also the number of hypertrophic chondrocytes was reduced by the treatment with 10 ng/ml FGF18 (vehicle treated: 152.67 ± 4.1 vs. FGF18 treated: 89.3 ± 1.45 cells) (Fig. 7B). Culturing with both 10^{-7} M CNP and 10 ng/ml FGF18 resulted in recovery by CNP of shortening of the growth plate in cultured mouse tibias by FGF18. Higher magnification of Alcian blue HE staining (Figs. 6C, D, G, H) and immunohistochemical staining for type X collagen (Figs. 6K, L) showed an increase in the hypertrophic chondrocyte layer compared with that of the FGF18-treated ones. The mean size of hypertrophic chondrocytes also increased compared with that of FGF18-treated ones (FGF18 treated: 314.01 ± 23.67 vs. CNP and FGF18 treated: 751.16 ± 41.6 μm^2) (Fig. 7A), and the reduction in number was also undone by CNP (FGF18 treated: 89.3 ± 1.45 vs. CNP and FGF18 treated: 145.3 ± 4.41 cells) (Fig. 7B).

Discussion

The study reported here used two different experimental designs to examine the interaction of the CNP/GC-B and FGFR-3 pathways in mouse chondrogenic ATDC5 cells and in organ-cultured tibias. In this study we were able to show that: (1) ATDC5 cells express GC-B, (2) FGF2 and FGF18 reduce CNP-dependent cGMP production in a dose-dependent manner without changing the amount of GC-B, (3) MAPK inhibitors attenuate the FGF inhibition of CNP-dependent cGMP production, (4) both CNP and cGMP inhibit the MAPK pathway but not the STAT-1 pathway of FGFR-3 activation without changing the amount of FGFR-3, and (5) CNP and FGF18 counteract longitudinal bone growth in organ cultured tibias.

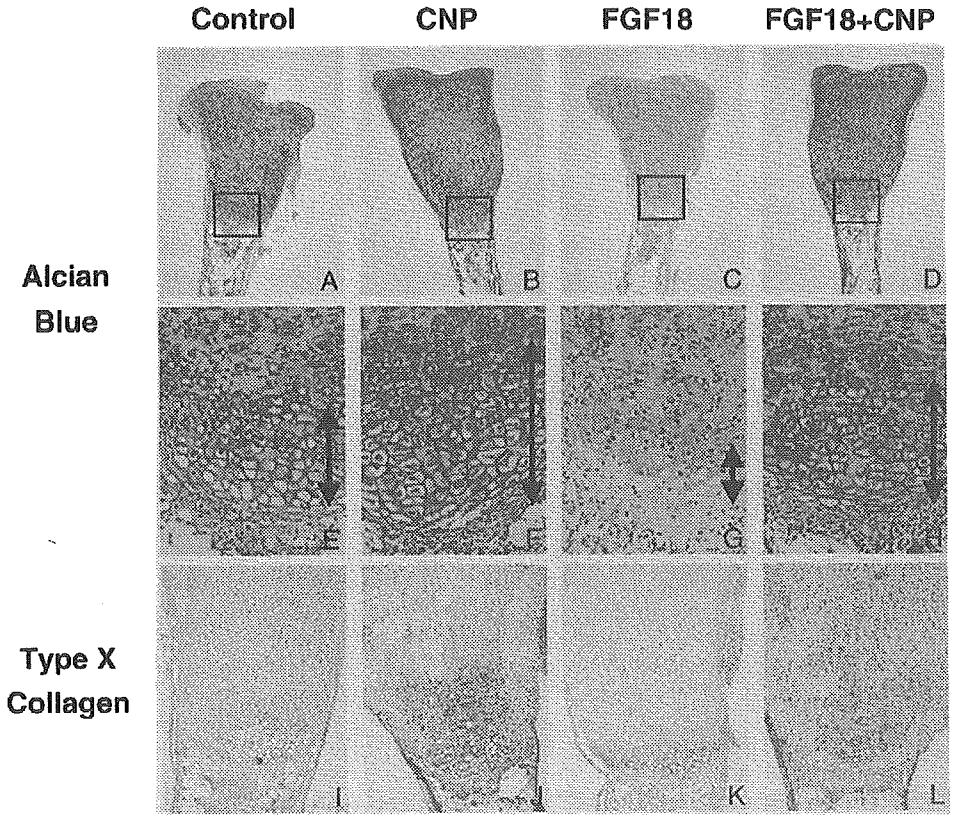

Fig. 6. Effect of CNP and FGF18 on mouse fetal tibia organ culture. Alcian blue and hematoxylin–eosin staining (upper and middle panels), and immunohistochemical staining for type X collagen (bottom panel) of cultured tibiae with CNP and/or FGF18. A, E, I: control; B, F, J: 10^{-7} M CNP; C, G, K: 10 ng/ml FGF18; D, H, L: 10 ng/ml FGF18 and 10^{-7} M CNP. Arrows indicate the hypertrophic chondrocyte zone. (A–D: magnification ×4, E–H: magnification ×20, I–L: magnification ×10.)

Substantial evidence exists that CNP is an antagonist of mitogenic action in many cell types. Activation of the CNP/GC-B pathway in the vascular smooth muscle cells was found to attenuate the onset of DNA synthesis, diminish cell proliferation, and inhibit chemotaxis [18]. As for the interaction of CNP with FGF signaling, marked elevation of cGMP induced by CNP had been reported to block the activation of the MAPK cascade induced by FGFs in fibroblast [19]. These indicate that significant antagonistic interplay may also occur between the CNP/GC-B pathway and growth factor-regulated pathways in growth plate chondrocytes.

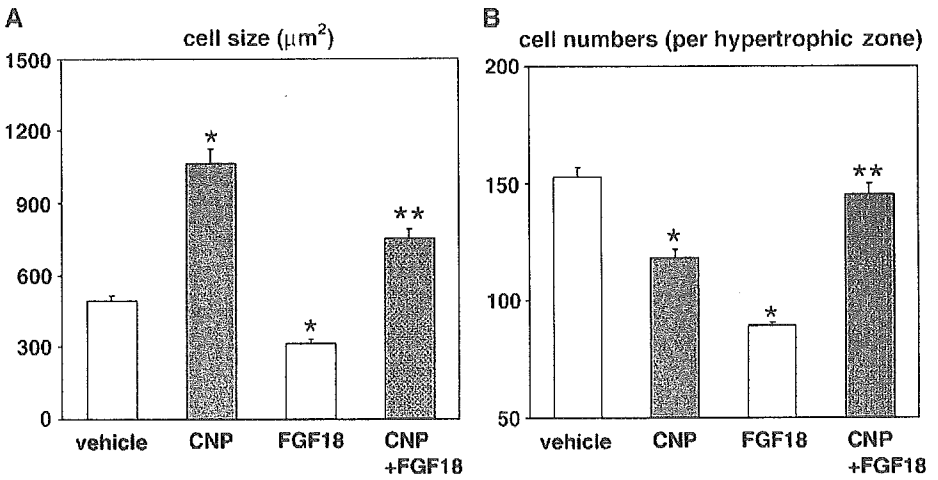

Fig. 7. Effect of CNP and FGF18 on mouse fetal tibia organ culture. (A) Effect of CNP and FGF18 on the size of hypertrophic chondrocytes (n = 10). Columns represent means ± SE (n = 10, each), *P < 0.01 vs. vehicle, **P < 0.01 vs. FGF18. (B) Effect of CNP and FGF18 on the numbers of hypertrophic chondrocytes (n = 5). Columns represent means ± SE (n = 5, each), *P < 0.01 vs. vehicle, **P < 0.01 vs. FGF18.

Constitutive activation of FGFR-3 has been reported to inhibit the proliferation and differentiation of the growth plate chondrocytes [20]. Our study clarified that CNP can undo the reduction in the size and numbers of chondrocytes of the hypertrophic zone of the growth plate of mouse tibias expressing the type X collagen, and compensate for the shortening of the growth plate resulting from the treatment with FGF18. These results are consistent with the findings of previous in situ hybridization studies which have shown that the mouse *fgfr-3* gene is widely expressed in the proliferative and prehypertrophic chondrocyte zones of cartilage [20], thus, overlapping the CNP/GC-B expression described in a previous study of ours [3]. Therefore, the interaction between the CNP/GC-B and FGFR-3 pathways in these cells results in the change of the hypertrophic chondrocytes during the endochondral ossification in the growth plate.

These findings, together with the fact that the specific MAPK inhibitors eliminated the FGF2-inhibition of CNP-dependent cGMP production in ATDC5 cells, suggest that the CNP/GC-B pathway and MAPK pathway counteracts through FGFR-3 in the regulation of growth plate chondrocytes.

Alternatively, one can hypothesize that the MAPK pathway is not the only FGFR-3 signaling pathway in chondrocytes. It has been suggested that the inhibitory effects of FGFs on bone growth are mediated by the STAT-1 pathway of FGFR-3 signaling [21], while a highly controlled balance between the MAPK and STAT-1 pathways has been demonstrated recently in growth factor-stimulated cells. The observation that the *Stat-1* null mice with overexpressing FGF2 can overcome apoptosis and the reduction in chondrocyte proliferation gives support to the view that the Stat-1 pathway may also have a key function in growth retardation [22]. In keeping with these findings, however, our observation of a significant ligand-independent STAT-1 phosphorylation in ATDC5 cells and no change in the level of STAT-1 phosphorylation as a result of stimulation by FGFs, CNP, or cGMP, leads us to conclude that the mechanism by which CNP undoes the shortening of bone length treated by FGFs consists of overcoming the MAPK-mediated pathway, not the STAT-1-mediated pathway.

Constitutive activation of ERK1 in chondrocytes reportedly induces a condition resembling achondroplasia [23]. Many studies have shown that activating mutations in FGFR-3 inhibit bone growth in patients with achondroplasia and thanatophoric dysplasia [24,25], while overexpression of FGF2 in mice slows longitudinal growth [26] and inactivating knockout mutations in FGFR-3 increase longitudinal long bone growth in mice [5]. On the other hand, CNP null mice as well as GC-B null mice are characterized by short stature with a phenotype histologically similar to that of achondroplasia [27]. Recently, we have shown that achondroplasia model mice, expressing the constitutive active mutant form of FGFR-3 (G380R) in cartilage [5], recovered from abnormal growth plate development and dwarfing phenotype as a result of the overexpression of CNP in their cartilage [28], suggesting that interaction between the CNP/GC-B and FGFR-3 pathways also occurs in vivo. Although two pathways are antagonistic, the effect of the CNP/GC-B pathway can overcome the effect of FGFR-3 pathway, partly because the activation level of downstream signaling of FGFR-3 (G380R) mutant is relatively weak [26], compared to the overexpressed CNP. During the course of this study, mutations in the human GC-B gene were reported to cause acromesomelic dysplasia, type Maroteaus, a type of skeletal dysplasia [29]. Therefore, the CNP/GC-B pathway appears critical for the proper progression of endochondral ossification also in human bone.

The downstream of the interaction between CNP/GC-B/cGMP pathway and FGFR-3/MAPK pathway remains unexplored. We recently reported that cGMP-dependent kinase depleted mice ($Prkg2^{-/-}$) showed abnormal growth plate development and dwarfing phenotype, that these changes were not affected by the overexpression of CNP in cartilage [30] and that the growth plate chondrocyte differentiation was disorganized, which is different from what has been observed in CNP-depleted mice.

GC-B is constitutively phosphorylated while receptor phosphorylation is absolutely essential for hormonal activation. On the other hand, the dephosphorylation of GC-B in response to hormone binding has been shown to correlate with the declining activity of these receptors in whole cells, suggesting that receptor dephosphorylation mediates the homologous desensitization of the receptor [31]. As the expression level of GC-B was not changed by FGF18 stimulation in our study, this dephosphorylation process may be involved in the desensitization of GC-B after FGFR-3 stimulation.

The clearance receptor of the natriuretic peptide reportedly mediates antimitogenic action of CNP in some but not all cell lines [32]. To determine if the effects of CNP were mediated by the clearance receptor in the ATDC5 cells, C-ANF, a selective ligand for the clearance receptor, was tested on ATDC5 cells and did not inhibit basal or FGF-stimulated ERK1/2 phosphorylation (data not shown).

We have demonstrated that the CNP/GC-B pathway engages in negative cross talks with FGFR pathways, that FGFs reduce CNP-dependent intracellular cGMP production and that CNP and cGMP markedly diminish the FGF-induced phosphorylation of ERK1/2 in chondrocytes. We also showed that CNP does not affect the amount of phosphorylated STAT-1 in chondrocytes. The results of our study show that FGFs and the activity of MAPK play an important role in the growth of chondrocytes, and negatively interact with the CNP/GC-B pathway and explain one of the molecular mechanisms of the growth stimulating action of CNP, suggesting that activation of the CNP/GC-B pathway may be effective for the treatment of achondroplasia.

Acknowledgments

This work was in part supported by Grant-in-Aid from The Ministry of Health, Labour and Welfare (#1028009) and the grant from the Smoking Research Foundation.

References

[1] Nakao K, Ogawa Y, Suga S, Imura H. Molecular biology and biochemistry of the natriuretic peptide system: I. natriuretic peptides. J Hypertens 1992;10:907–12.
[2] Nakao K, Ogawa Y, Suga S, Imura H. Molecular biology and biochemistry of the natriuretic peptide system: II. natriuretic peptide receptors. J Hypertens 1992;10:1111–4.
[3] Chusho H, Tamura N, Ogawa Y, Yasoda A, Suda M, Miyazawa T, et al. Dwarfism and early death in mice lacking C-type natriuretic peptide. Proc Natl Acad Sci USA 2001;98:4016–21.
[4] Yasoda A, Ogawa Y, Suda M, Tamura N, Mori K, Sakuma Y, et al. Natriuretic peptide regulation of endochondral ossification. Evidence for possible roles of the C-type natriuretic peptide/guanylyl cyclase-B pathway. J Biol Chem 1998;273:11695–700.
[5] Colvin JS, Bohne BA, Harding GW, McEwen DG, Ornitz DM. Skeletal overgrowth and deafness in mice lacking fibroblast growth factor receptor 3. Nat Genet 1996;4:390–7.
[6] Kanai M, Goke M, Tsunekawa S, Podolsky DK. Signal transduction pathway of human fibroblast growth factor receptor 3. Identification of a novel 66-kDa phosphoprotein. J Biol Chem 1997;272:6621–8.
[7] Deng C, Wynshaw-Boris A, Zhou F, Kuo A, Leder P. Fibroblast growth factor receptor 3 is a negative regulator of bone growth. Cell 1996;84:911–21.
[8] Tavormina PL, Rimoin DL, Thompson LM, Zhu YZ, Wilkin DJ, Lachman RS, et al. Thanatophoric dysplasia (type I and II) caused by distinct mutations in fibroblast growth factor receptor 3. Nat Genet 1995;9:321–8.
[9] Shimizu A, Tada K, Shukunami C, Hiraki Y, Kurokawa T, Magane N, et al. A novel alternatively spliced fibroblast growth factor receptor 3 isoform lacking the acid box domain is expressed during chondrogenic differentiation of ATDC5 cells. J Biol Chem 2001;276: 11031–40.
[10] Ellsworth JL, Berry J, Bukowski T, Claus J, Feldhaus A, Holderman S, et al. Fibroblast growth factor-18 is a trophic factor for mature chondrocytes and their progenitors. Osteoarthr Cartil 2002;10:308–20.
[11] Ohbayashi N, Shibayama M, Kurotaki Y, Imanishi M, Fujimori T, Itoh N, et al. FGF18 is required for normal cell proliferation and differentiation during osteogenesis and chondrogenesis. Genes Dev 2002; 16:870–9.
[12] Liu Z, Xu J, Colvin JS, Ornitz DM. Coordination of chondrogenesis and osteogenesis by fibroblast growth factor 18. Genes Dev 2002; 16:859–69.
[13] Shukunami C, Shigeno C, Atsumi T, Ishizeki K, Suzuki F, Hiraki Y. Chondrogenic differentiation of clonal mouse embryonic cell line ATDC5 in vitro: differentiation-dependent gene expression of parathyroid hormone (PTH)/PTH-related peptide receptor. J Cell Biol 1996;133:457–68.
[14] Suda M, Tanaka K, Yasoda A, Komatsu Y, Chusho H, Miura M, et al. C-type natriuretic peptide/guanylate cyclase B system in ATDC5 cells, a chondrogenic cell line. J Bone Miner Metab 2002;20:136–41.
[15] Tamura N, Garbers DL. Regulation of the guanylyl cyclase-B receptor by alternative splicing. J Biol Chem 2003;278:48880–9.
[16] Miura M, Tanaka K, Komatsu Y, Suda M, Yasoda A, Sakuma Y, et al. Thyroid hormones promote chondrocyte differentiation in mouse ATDC5 cells and stimulate endochondral ossification in fetal mouse tibias through iodothyronine deiodinases in the growth plate. J Bone Miner Metab 2002;17:443–54.
[17] Hotokezaka H, Sakai E, Kanaoka K, Saito K, Matsuo K, Kitaura H, et al. U0126 and PD98059, specific inhibitors of MEK, accelerate differentiation of RAW264.7 cells into osteoclast-like cells. J Biol Chem 2002;277:47366–72.
[18] Komatsu Y, Itoh H, Suga S, Ogawa Y, Hama N, Kishimoto I, et al. Regulation of endothelial production of C-type natriuretic peptide in coculture with vascular smooth muscle cells. Role of the vascular natriuretic peptide system in vascular growth inhibition. Circ Res 1996;78:606–14.
[19] Chrisman TD, Garbers DL. Reciprocal antagonism coordinates C-type natriuretic peptide and mitogen-signaling pathways in fibroblasts. J Biol Chem 1999;274:4293–9.
[20] Naski MC, Colvin JS, Coffin JD, Ornitz DM. Repression of hedgehog signaling and BMP4 expression in growth plate cartilage by fibroblast growth factor receptor 3. Development 1998;125:4977–88.
[21] Sahni M, Ambrosetti DC, Mansukhani A, Gertner R, Levy D, Basilico C. FGF signaling inhibits chondrocyte proliferation and regulates bone development through the STAT-1 pathway. Genes Dev 1999; 13:1361–6.
[22] Sahni M, Raz R, Coffin JD, Levy D, Basilico C. STAT1 mediates the increased apoptosis and reduced chondrocyte proliferation in mice overexpressing FGF2. Development 2001;128:2119–29.
[23] Murakami S, Balmes G, McKinney S, Zhang Z, Givol D, de Crombrugghe B. Constitutive activation of MEK1 in chondrocytes causes Stat1-independent achondroplasia-like dwarfism and rescues the Fgfr3-deficient mouse phenotype. Genes Dev 2004;18:290–305.
[24] Shiang R, Thompson LM, Zhu YZ, Church DM, Fielder TJ, Bocian M, et al. Mutations in the transmembrane domain of FGFR3 cause the most common genetic form of dwarfism, achondroplasia. Cell 1994; 78:335–42.
[25] Webster MK, D'Avis PY, Robertson SC, Donogue DJ. Profound ligand-independent kinase activation of fibroblast receptor 3 by the activation loop mutation responsible for a lethal skeletal dysplasia, thanatophoric dysplasia type II. Mol Cell Biol 1996;16:4081–7.
[26] Coffin JD, Florkiewicz RZ, Neumann J, Mort-Hopkins T, Dorn II GW, Lightfoot P, et al. Abnormal bone growth and selective translational regulation in basic fibroblast growth factor (FGF-2) transgenic mice. Mol Biol Cell 1995;6:1861–73.
[27] Tamura N, Doolittle LK, Hammer RE, Shelton JM, Richardson JA, Garbers DL. Critical roles of the guanylyl cyclase B receptor in endochondral ossification and development of female reproductive organs. Proc Natl Acad Sci USA 2004;101:17300–5.
[28] Yasoda A, Komatsu Y, Chusho H, Miyazawa T, Ozasa A, Miura M, et al. Overexpression of CNP in chondrocytes rescues achondroplasia through a MAPK-dependent pathway. Nat Med 2004;10:80–6.
[29] Bartels CF, Bukulmez H, Padayatti P, Rhee DK, van Ravenswaaij-Arts C, Pauli RM, et al. Mutations in the transmembrane natriuretic peptide receptor NPR-B impair skeletal growth and cause acromesomelic dysplasia, type Maroteaux. Am J Hum Genet 2004;75: 27–34.
[30] Miyazawa T, Ogawa Y, Chusho H, Yasoda A, Tamura N, Komatsu Y, et al. Cyclic GMP-dependent protein kinase II plays a critical role in C-type natriuretic peptide-mediated endochondral ossification. Endocrinology 2002;143:3604–10.
[31] Abbey SE, Potter LR. Lysophosphatidic acid inhibits C-type natriuretic peptide activation of guanylyl cyclase-B. Endocrinology 2003;144:240–6.
[32] Komatsu Y, Itoh H, Suga S, Igaki T, Ogawa Y, Kishimoto I, et al. Regulation of secretion and clearance of C-type natriuretic peptide in the interaction of vascular endothelial cells and smooth muscle cells. J Hypertens 1996;14:585–92.

THE JOURNAL OF BIOLOGICAL CHEMISTRY
Vol. 280, No. 15, Issue of April 15, pp. 15247–15256, 2005
Printed in U.S.A.

Analysis of Rat Insulin II Promoter-Ghrelin Transgenic Mice and Rat Glucagon Promoter-Ghrelin Transgenic Mice*

Received for publication, October 5, 2004, and in revised form, February 3, 2005
Published, JBC Papers in Press, February 8, 2005, DOI 10.1074/jbc.M411358200

Hiroshi Iwakura‡, Kiminori Hosoda‡§, Choel Son‡, Junji Fujikura‡, Tsutomu Tomita‡, Michio Noguchi‡, Hiroyuki Ariyasu‡, Kazuhiko Takaya‡‖, Hiroaki Masuzaki‡, Yoshihiro Ogawa‡, Tatsuya Hayashi‡, Gen Inoue‡, Takashi Akamizu‖, Hiroshi Hosoda‖, Masayasu Kojima‡‡, Hiroshi Itoh‡, Shinya Toyokuni¶, Kenji Kangawa‖**, and Kazuwa Nakao‡**

*From the ‡Department of Medicine and Clinical Science, Endocrinology and Metabolism and ¶Department of Pathology and Biology of Diseases, Kyoto University Graduate School of Medicine, 54 Shogoin Kawahara-cho, Sakyo-ku, Kyoto 606-8507, the ‖Translational Research Center, Kyoto University Hospital, Kyoto 606-8507, the ‡‡Department of Molecular Genetics, Institute of Life Science, Kurume University, Fukuoka 839-0861, and the **Department of Biochemistry, National Cardiovascular Center Research Institute, Osaka 565-8565, Japan*

We developed and analyzed two types of transgenic mice: rat insulin II promoter-ghrelin transgenic (RIP-G Tg) and rat glucagon promoter-ghrelin transgenic mice (RGP-G Tg). The pancreatic tissue ghrelin concentration measured by C-terminal radioimmunoassay (RIA) and plasma desacyl ghrelin concentration of RIP-G Tg were about 1000 and 3.4 times higher than those of nontransgenic littermates, respectively. The pancreatic tissue *n*-octanoylated ghrelin concentration measured by N-terminal RIA and plasma *n*-octanoylated ghrelin concentration of RIP-G Tg were not distinguishable from those of nontransgenic littermates. RIP-G Tg showed suppression of glucose-stimulated insulin secretion. Arginine-stimulated insulin secretion, pancreatic insulin mRNA and peptide levels, β cell mass, islet architecture, and GLUT2 and PDX-1 immunoreactivity in RIP-G Tg pancreas were not significantly different from those of nontransgenic littermates. Islet batch incubation study did not show suppression of insulin secretion of RIP-G Tg *in vitro*. The insulin tolerance test showed lower tendency of blood glucose levels in RIP-G Tg. Taking lower tendency of triglyceride level of RIP-G Tg into consideration, these results may indicate that the suppression of insulin secretion is likely due to the effect of desacyl ghrelin on insulin sensitivity. RGP-G Tg, in which the pancreatic tissue ghrelin concentration measured by C-RIA was about 50 times higher than that of nontransgenic littermates, showed no significant changes in insulin secretion, glucose metabolism, islet mass, and islet architecture. The present study raises the possibility that desacyl ghrelin may have influence on glucose metabolism.

Ghrelin is a 28-amino acid peptide with unique modification of acylation, which is essential for its biological action (1). Ghrelin was originally identified in rat stomach as an endogenous ligand for an orphan receptor, which has been so far called growth hormone secretagogue receptor (GHS-R)[1] (1). Ghrelin expression is detected in the stomach, intestine, hypothalamus, pituitary gland, kidney, placenta, and testis (2–6). Ghrelin is involved in a wide variety of the functions, including the regulation of growth hormone release, food intake, gastric acid secretion, gastric motility, blood pressure, and cardiac output (7–19).

Recently Date *et al.* (20) reported that ghrelin is present in α cells of normal human and rat pancreatic islets. Volante *et al.* (21) described ghrelin-expression in β cells of human islet. Wierup *et al.* and Prado *et al.* reported that ghrelin-expressing cells are a new islet cell type distinct from α, β, δ, and PP cells in human, rat, and mouse islets (22–24). Although there was no apparent change of plasma insulin levels in ghrelin null mouse (25, 26), which may indicate that ghrelin is not a direct regulator of insulin secretion in the physiological condition, there have been several reports of the effect of pharmacological dose of ghrelin on insulin secretion. Broglio *et al.*, Egido *et al.*, and Reimer *et al.* have reported that ghrelin has an inhibitory effect on insulin secretion (27–30). Adeghate *et al.*, Date *et al.*, and Lee *et al.* have reported that ghrelin stimulates insulin secretion (20, 31, 32). Salehi *et al.* have reported ghrelin has both inhibitory and stimulatory effects depending on its concentration (33). Therefore, there is still a lot of controversy about the localization of ghrelin in the pancreas and the effects of ghrelin on the insulin secretion. As for the effects of desacyl ghrelin on insulin secretion, Broglio *et al.* (34) have reported that acute desacyl ghrelin administration has no effect on insulin secretion in human but that it counteracts the inhibitory effect of *n*-octanoylated ghrelin on insulin secretion when co-administrated with *n*-octanoylated ghrelin (35).

Here we developed and analyzed two types of transgenic mice: rat insulin II promoter-ghrelin transgenic mice (RIP-G Tg) and rat glucagon promoter-ghrelin transgenic mice (RGP-G Tg). The purpose of this study was to clarify the effect of transgenic overexpression of ghrelin cDNA in pancreatic islets.

EXPERIMENTAL PROCEDURES

Generating RIP- and RGP-ghrelin Transgenic Mice—Mouse stomach cDNA library was constructed from 1 μg of mouse stomach poly(A)$^+$

* This work was supported by research grants from the Japanese Ministry of Education, Culture, Sports, Science and Technology, the Japanese Ministry of Health, Labor and Welfare. The costs of publication of this article were defrayed in part by the payment of page charges. This article must therefore be hereby marked "*advertisement*" in accordance with 18 U.S.C. Section 1734 solely to indicate this fact.

§ To whom correspondence should be addressed. Tel.: 81-75-751-3172; Fax: 81-75-771-9452; E-mail: kh@kuhp.kyoto-u.ac.jp.

[1] The abbreviations used are: GHS-R, growth hormone secretagogue receptor; RIP-G Tg, rat insulin II promoter-ghrelin transgenic; RGP-G Tg, rat glucagon promoter-ghrelin transgenic mice; RIA, radioimmunoassay; C-RIA, anti-ghrelin [13–28] antiserum; N-RIA, anti-ghrelin [1–11] antiserum; RT, reverse transcription; HDL, high density lipoprotein; PP, pancreatic polypeptide.

RNA with a cDNA synthesis kit (Amersham Biosciences). Mouse ghrelin cDNA was isolated from this library, using rat ghrelin cDNA as a probe. A fusion gene comprising RIP and mouse ghrelin cDNA coding sequences was designed. The purified fragment (10 μg/ml) was microinjected into the pronucleus of fertilized C57/B6J mice (SLC, Shizuoka, Japan) eggs. The viable eggs were transferred into the oviducts of pseudopregnant female ICR mice (SLC) using standard techniques. Transgenic founder mice were identified by Southern blot analysis of tail DNAs using the mouse ghrelin cDNA fragment as a probe. RGP-G Tg was generated similarly. Transgenic mice were used as heterozygotes. Animals were maintained on standard rat food (CE-2, 352 kcal/100 g, Japan CLEA, Tokyo, Japan) on a 12-h light/12-h dark cycle. All experimental procedures were approved by the Kyoto University Graduate School of Medicine Committee on Animal Research.

Immunohistochemistry—Formalin-fixed, paraffin-embedded tissue sections were immunostained using the avidin-biotin peroxidase complex method (Vectastain "ABC" Elite kit, Vector Laboratories, Burlingame, CA) as described previously (36). Serial sections were used, and the thickness of each section was 5 μm. Sections were incubated with anti-C-terminal ghrelin [13–28] (1:1000 at final dilution), anti-N-terminal ghrelin [1–11] (1:2000) (1), which recognizes the *n*-octanoylated portion of ghrelin, anti-glucagon (1:500), anti-insulin (1:500), anti-somatostatin (1:500), anti-pancreatic polypeptide (PP, 1:500, DAKO, Glostrup, Denmark), anti-PDX-1 (1:2000, kindly provided by Christopher V. E. Wright) (37), and anti-GLUT2 (1:200, kindly provided by Bernard Thorens) (38) antisera. Quantification of β cell area was performed in insulin-stained sections by using Axio Vision (Carl Zeiss, Hallbergmoos, Germany) and Scion Image (Scion Corp., Frederick, MD). Ten sections (200-μm interval) for each mouse ($n = 5$) were analyzed. The percentage of β cell area in the pancreas was determined by dividing the area of all insulin-positive cells in one section by the total area of the section.

Measurements of Plasma and Tissue Ghrelin Concentrations—Plasma was sampled from 10-week-old RIP-G Tg and their nontransgenic littermates under ad libitum feeding states considering the promoter activity. From RGP-G Tg and their littermates, it was sampled after overnight fast. Blood was withdrawn from the retroorbital vein or the proximal end of the portal vein under ether anesthesia, immediately transferred to chilled siliconized glass tubes containing Na_2EDTA (1 mg/ml) and aprotinin (1000 KIU/ml, Ohkura Pharmaceutical, Kyoto, Japan), and centrifuged at 4 °C. Hydrogen chloride was added to the samples at a final concentration of 0.1 N immediately after separation of plasma. Plasma was immediately frozen and stored at −80 °C until assay. Plasma ghrelin concentration was determined by desacyl ghrelin enzyme-linked immunosorbent assay kit and active-ghrelin enzyme-linked immunosorbent assay kit that recognizes *n*-octanoylated ghrelin (Mitsubishi Kagaku Iatron, Tokyo, Japan).

As for measurement of tissue ghrelin concentration, pancreata or stomachs were taken from the 8-week-old male mice. The rumen was removed from the stomach. Samples were diced and boiled for 5 min in the 10-fold v/w of water. Acetic acid was added to each solution so that the final concentration was adjusted to 1 M, and the tissues were homogenized. The supernatants were obtained after centrifugation. Tissue ghrelin concentration was determined by radioimmunoassay (RIA) using anti-ghrelin [13–28] antiserum (C-RIA) and anti-ghrelin [1–11] antiserum (N-RIA) as described previously (39).

Measurements of Body Weight and Food Consumption—Mice were housed individually and were allowed free access to standard rat chow. Body weights of mice were measured weekly. Daily food intake was measured by weighing the pellets between 9:00 and 10:00 a.m.

Measurements of % Body Fat and Visceral/Subcutaneous Fat Mass Ratio—Forty-week-old mice were anesthetized with pentobarbital. Percent body fat and visceral/subcutaneous fat mass ratio of mice were measured by Latheta LTC-100 (ALOKA, Tokyo, Japan).

Glucose and Insulin Tolerance Tests—For the glucose tolerance test, after overnight fast, the mice were injected with 1.5 g/kg glucose intraperitoneally. For the insulin tolerance test, after a 4-h fast, mice were injected with 2.0 milliunits/g human regular insulin (Novolin R; Novo Nordisk, Bagsvaerd, Denmark) intraperitoneally. Blood was sampled from the tail vein before and 15, 30, 60, 90, and 120 min after the injection. Blood glucose levels were determined by glucose oxidase method using Glutest sensor (Sanwa Kagaku, Kyoto, Japan).

Insulin Release—After overnight fast, the mice were injected with 3.0 g/kg glucose or 0.25 g/kg L-arginine intraperitoneally. Plasma was sampled from the tail vein before and 2, 5, 15, 30, and 60 min after the injection using heparin coated tubes. The measurement of insulin concentration was carried out by enzyme-linked immunosorbent assay using ultra-sensitive rat insulin kit (Morinaga, Yokohama, Japan).

Pancreatic Insulin Concentration—As for measurement of pancreatic insulin concentration, pancreata were obtained from the mice under the ether anesthesia and homogenized in acid-ethanol. The supernatants were used for assay after centrifugation.

Batch Incubation of Islet—Under the pentobarbital anesthesia, Type IV collagenase (Worthington, Lakewood, NJ) dissolved in Hanks' balanced salt solution (1.5 mg/ml) was injected into mouse pancreatic duct. Pancreas was removed and incubated at 37 °C for 14 min. After washing out collagenase by Hanks' balanced salt solution, islets were collected by Ficoll gradient and manually picked up so that the sizes of the islets were equal. Islets were incubated at 37 °C in RPMI1640 containing 10% fetal calf serum for 2 h and then in Krebs-Ringer bicarbonate buffer containing 3.3 mM glucose and 0.2% bovine serum albumin for 30 min. Five islets were incubated at 37 °C in 500 μl of Krebs-Ringer bicarbonate buffer containing 0.2% bovine serum albumin and 3.3 or 8.7 or 16.7 mM glucose for 1 h. After centrifugation, the supernatants were collected. Insulin concentrations in supernatants were determined by rat insulin kit (Morinaga, Yokohama, Japan).

Northern Blot Analysis and Real-time Quantitative RT-PCR—Total RNA was extracted from pancreata using RNeasy mini kit (Qiagen K.K., Tokyo, Japan). Filters containing 5 μg of total RNA were prepared. Northern blot analyses were performed as described previously (36) using the mouse insulin II cDNA and human β-actin cDNA (Clontech, Palo Alto, CA) as probes. To confirm that approximately equal amounts of total RNA were assayed in Northern blot hybridization analysis, the density of 18 S rRNA in the gel and signal of β-actin in each lane was used. The hybridization signal intensity was quantitated using an image analyzer BAS-2500 (Fuji Photo Film, Tokyo, Japan). Reverse transcription (RT) was performed with random hexamer and Super-Script II reverse transcriptase (Invitrogen). Real-time quantitative PCR was performed with ABI PRISM 7700 Sequence Detection System (Applied Biosystems, Foster City, CA). The following primers and TaqMan probes were used: mouse GHS-R (sense, 5′-CACCAACCTCT-ACCTATCCAGCAT-3′; antisense, 5′-CTGACAAACTGGAAGAGTTTG-CA-3′; TaqMan probe, 5′-TCCGATCTGCTCATCTTCCTGTGCATG-3′); mouse ghrelin (sense, 5′-GCATGCTCTGGATGGACATG-3′; antisense, 5′-TGGTGGCTTCTTGGATTCCT-3′; TaqMan probe, 5′-AGCCCAGA-GCACCAGAAAGCCCA-3′).

Lipid Measurements—Blood was collected from the retroorbital vein of 35-week-old RIP-G Tg and their nontransgenic littermates. After separation of serum, total cholesterol, triglyceride, free fatty acid, and HDL-cholesterol levels in serum were determined by Cholesterol E-test Wako, Triglyceride E-test Wako, NEFA C-test Wako, and HDL-cholesterol E-test Wako (Wako Pure Chemical Industries, Osaka, Japan).

Statistical Analysis—All values were expressed as means ± S.E. Statistical significance of difference in mean values was assessed by repeated measures analysis of variance or Student's *t* test.

RESULTS

Distribution of Ghrelin in Normal Mouse Pancreas—We first examined which cell type of islet cells expresses ghrelin in mouse by immunohistochemistry using anti-C-terminal ghrelin antiserum. In the most of the islets no ghrelin-like immunoreactivity was detected. C-terminal ghrelin-like immunoreactivity was observed in the periphery of minor proportion of islets of wild type mice (Fig. 1*A*). Most of the ghrelin-positive cells were also glucagon-positive by serial section analysis (Fig. 1*B*), whereas most of the glucagon-positive cells were not ghrelin-positive.

Generation of RIP- and RGP-ghrelin Transgenic Mice—A fusion gene comprising RIP and mouse ghrelin cDNA coding sequences was designed so that ghrelin expression might be targeted to the pancreatic β cells (Fig. 2*A*). The ghrelin mRNA level of RIP-G Tg in pancreas determined by quantitative RT-PCR was about 215 times higher than that of nontransgenic littermates (215.3 ± 40.6 *versus* 1.0 ± 0.025 arbitrary units, $n = 5$, $p < 0.01$). There was also an increase in ghrelin mRNA levels in brain of RIP-G Tg (242.6 ± 17.6 *versus* 89.1 ± 27.3 arbitrary unit, $n = 5$, $p < 0.01$). To confirm the expression of ghrelin transgene in pancreatic β cells, we performed an immunohistochemical analysis using anti-C-terminal ghrelin antiserum. C-terminal ghrelin-like immunoreactivity was observed in the nearly whole area of the islets of the RIP-G Tg (Fig. 2*C*), whereas it was only seen in the periphery of the islets

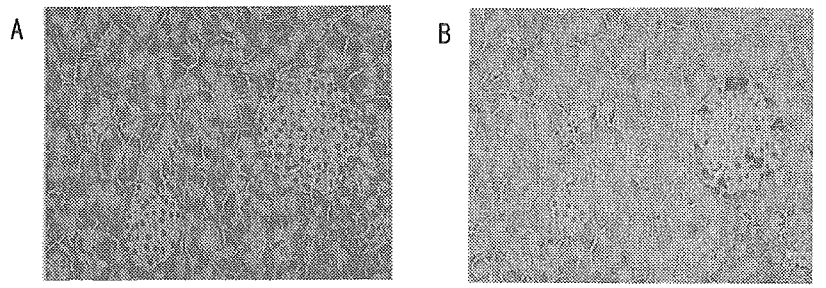

FIG. 1. *A*, C-terminal ghrelin-like immunoreactivity in adult mouse islet. The staining was observed in the peripheral region of the islet. *B*, glucagon-like immunoreactivity in serial section.

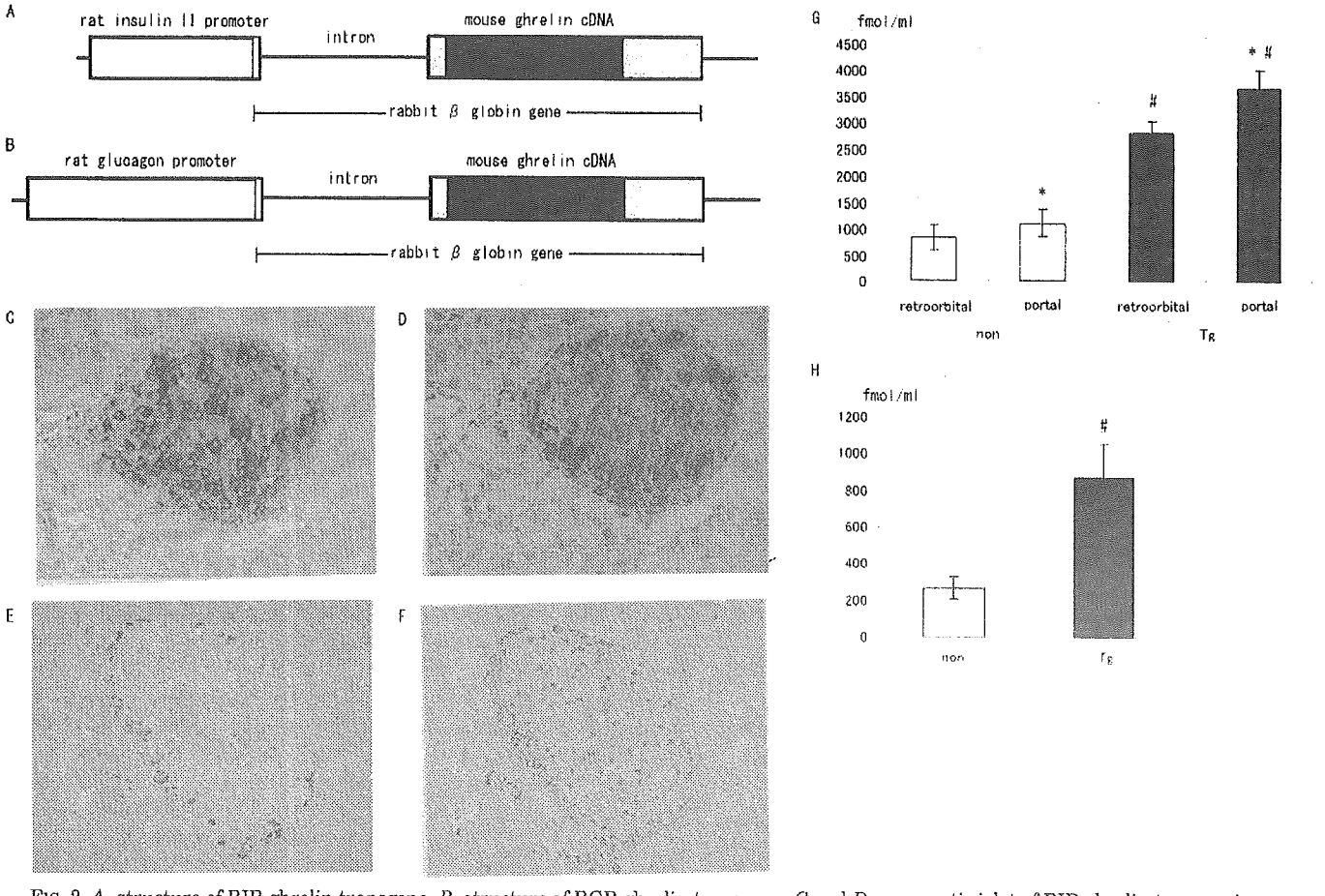

FIG. 2. *A*, structure of RIP-ghrelin transgene. *B*, structure of RGP-ghrelin transgene. *C* and *D*, pancreatic islet of RIP-ghrelin transgenic mouse stained with anti-C-terminal ghrelin (*C*) and anti-N-terminal ghrelin antisera (*D*). *E* and *F*, pancreatic islet of RGP-ghrelin transgenic mouse stained with anti-C-terminal ghrelin (*E*) and anti-N-terminal ghrelin antisera (*F*). *G*, plasma ghrelin levels collected from retroorbital and portal veins in RIP-G Tg. *, $p < 0.05$ compared with retroorbital vein. #, $p < 0.01$ compared with nontransgenic littermates. *H*, the step-up of ghrelin concentration from retroorbital vein to portal vein in RIP-G Tg. #, $p < 0.01$ compared with their nontransgenic littermates.

of their nontransgenic littermates (Fig. 1*A*). Immunohistochemical analysis using anti-N-terminal ghrelin antiserum showed the same staining pattern (Fig. 2*D*), indicating that *n*-octanoylated ghrelin may be produced in β cells of this transgenic mouse. We also stained the brain section of RIP-G Tg. No ghrelin-like immunoreactivity was detected either with anti-C-terminal or anti-N-terminal ghrelin antisera (data not shown). The pancreatic tissue ghrelin concentration of RIP-G Tg measured by C-RIA was about 1000 times higher than that of their nontransgenic littermates (1024 ± 108.9 fmol/mg *versus* 1.2 ± 0.1 fmol/mg, $n = 5, p < 0.01$). This concentration was about one third of the nontransgenic stomach concentration (3558.1 ± 51.0 fmol/mg, $n = 5$). The pancreatic tissue ghrelin concentration of RIP-G Tg measured by N-RIA tended to be also higher than that of their nontransgenic littermates (0.054 ± 0.017 fmol/mg *versus* 0.038 ± 0.006fmol/mg, $n = 5$, NS; not significant), but it did not reach statistical significance. Plasma desacyl ghrelin concentration of RIP-G Tg was about 3.4 times higher than that of nontransgenic littermates under the ad libitum feeding states (2805.5 ± 236.4 *versus* 825.9 ± 244.4 fmol/ml, $n = 5, p < 0.01$, Fig. 2*G*). We also measured desacyl ghrelin levels in portal vein of the mice. In the nontransgenic mice, the portal desacyl ghrelin level was significantly higher than that in retroorbital vein (1108.0 ± 257.3 fmol/ml *versus* 825.9 ± 244.4 fmol/ml, $n = 5, p < 0.05$, Fig. 2*G*). The desacyl ghrelin concentration collected from portal vein of RIP-G Tg at the same time was much higher than that of nontransgenic littermates (3671.8 ± 328.6 *versus* 1108.0 ± 257.3 fmol/ml, $n = 5, p < 0.01$, Fig. 2*G*). The step-up of desacyl ghrelin concentration from retroorbital vein to portal vein of RIP-G Tg was significantly higher than that of nontransgenic littermates (866.3 ± 182.2 fmol/ml *versus* 262.9 ± 59.8 fmol/ml, $p < 0.01$, Fig. 2*H*). Plasma *n*-octanoylated ghrelin levels in retroorbital and portal vein of RIP-G Tg tended to be higher than those of their nontransgenic littermates (retroorbital: 78.5 ± 13.4 *versus* 66.1 ± 7.1 fmol/ml, $n = 5$, NS; portal: 104.6 ± 15.3 *versus*

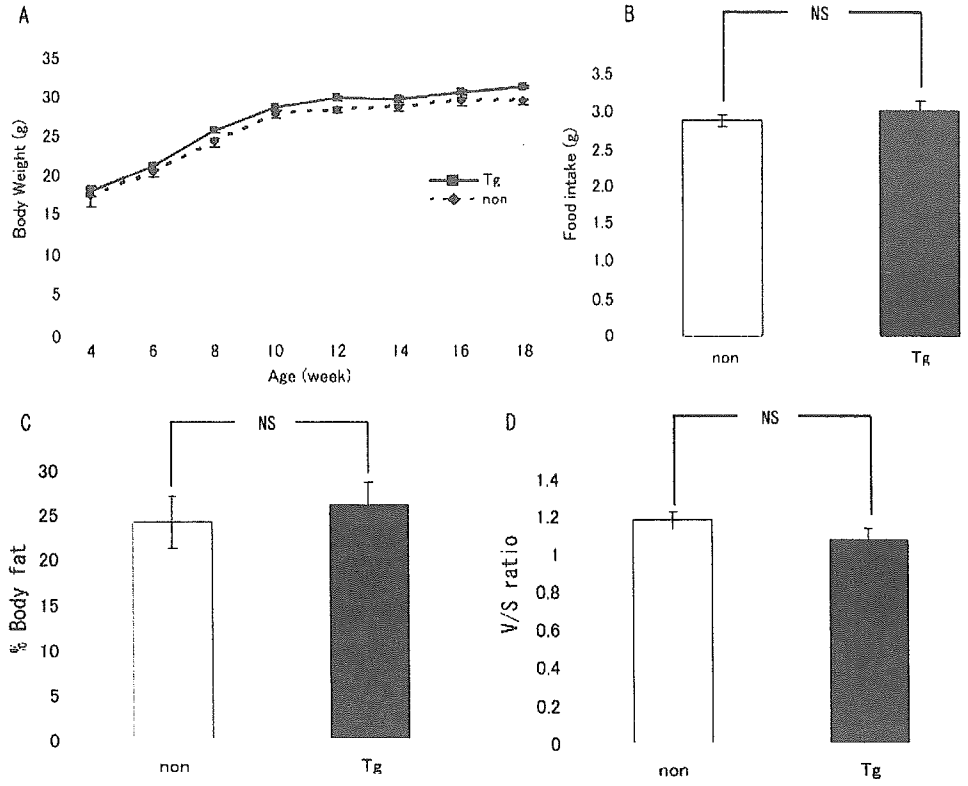

FIG. 3. *A*, body weight of RIP-G Tg (*Tg*) and their nontransgenic littermates (*non*). *B*, food intake of RIP-GTg (*Tg*) and their nontransgenic littermates (*non*). Percent body fat (*C*) and visceral/subcutaneous fat ratio (*D*) of RIP-GT$_g$ and their nontransgenic littermates (*non*).

71.4 ± 9.0 fmol/ml, n = 5, NS), but it did not reach statistical significance.

We also generated RGP-G Tg, in which ghrelin expression is targeted to the pancreatic α cells (Fig. 2*B*). The ghrelin mRNA level Tg in pancreas of RGP-G determined by quantitative RT-PCR was about 16 times higher than that of nontransgenic littermates (16.3 ± 1.7 *versus* 1.0 ± 0.24 arbitrary unit, n = 5, $p < 0.01$). The ghrelin mRNA level in duodenum of RGP Tg was not statistically different from that of nontransgenic littermates (520.1 ± 111.1 *versus* 379.1 ± 37.6 arbitrary unit, n = 5, NS). The ghrelin mRNA level in brain of RGP Tg was not distinguishable from that of nontransgenic littermates (72.0 ± 6.4 *versus* 71.8 ± 7.8 arbitrary unit, n = 5, NS). Immunohistochemical analysis showed ghrelin-like immunoreactivity in the periphery of the pancreatic islet of RGP-ghrelin transgenic mouse by both anti-C-terminal ghrelin and anti-N-terminal ghrelin antisera (Fig. 2, *E* and *F*). The pancreatic tissue ghrelin concentrations of RGP-G Tg measured by C-RIA were about 50 times higher than those of their nontransgenic littermates (48.9 ± 2.5 fmol/mg *versus* 1.2 ± 0.1 fmol/mg, n = 5, $p < 0.01$). The pancreatic tissue ghrelin concentration of RGP-G Tg measured by N-RIA tended to be higher than that of their nontransgenic littermates (0.076 ± 0.019 fmol/mg *versus* 0.038 ± 0.006 fmol/mg, n = 5, NS), but it did not reach statistical significance. The plasma desacyl ghrelin concentrations in retroorbital vein were not elevated in RGP-G Tg after over night fasting compared with nontransgenic littermates (661.6 ± 38.0 *versus* 1024.7 ± 27.1 fmol/ml, n = 5). The portal desacyl ghrelin concentrations of RGP-G Tg were also indistinguishable from those of their nontransgenic littermate (1320.6 ± 164.7 *versus* 1442.9 ± 361.5 fmol/ml, n = 5, NS). Plasma n-octanoylated ghrelin levels in retroorbital and portal vein of RGP-G Tg were indistinguishable from those of their nontransgenic littermates (retroorbital: 98.3 ± 18.7 *versus* 133.5 ± 25.3 fmol/ml, n = 5, NS; portal: 154.3 ± 20.7 *versus* 198.9 ± 34.9 fmol/ml, n = 5, NS).

Body Weight, Food Consumption, and Percent Body Fat—There was no significant difference in body weight and food intake between RIP-G Tg and their nontransgenic littermates (Fig. 3). Percent body fat and visceral/subcutaneous ratio of RIP-G Tg were not different from those of nontransgenic littermates (Fig. 2, *C* and *D*). No significant changes were observed in RGP-G Tg, either (data not shown).

Glucose Metabolism and Insulin Secretion—Although no significant differences in blood glucose levels were noted between RIP-G Tg and their nontransgenic littermates on the fasting state and intraperitoneal glucose tolerance tests (Fig. 4, *A* and *C*), plasma insulin levels 2 and 30 min after the glucose injection were significantly decreased in RIP-G Tg compared with those in their nontransgenic littermates (Fig. 4*D*). Suppression of insulin secretion was not observed in RIP-G Tg on intraperitoneal injection of arginine (Fig. 4*G*). Blood glucose level of RIP-G Tg in the insulin tolerance test tended to be lower than those of their nontransgenic littermates, but it did not reach statistical significance (Fig. 4*H*).

No significant differences in blood glucose or insulin levels were observed between RGP-G Tg and their nontransgenic littermates on the fasting state, ad libitum feeding, or intraperitoneal glucose or arginine injection (Fig. 4, *B*, *E*, and *F*, and data not shown). Blood glucose levels on insulin tolerance test showed no differences between RGP-ghrelin and their nontransgenic littermates (data not shown).

Islet Architecture and β Cell Mass—We studied the tissue sections of RIP-G Tg to explore the effect of ghrelin on the islet architecture and β cell mass. There were no obvious abnormalities in the intra islet cytoarchitecture and cell number of insulin, glucagon, somatostatin, and PP cells in the islets of the RIP-G Tg (Fig. 5*A–D*). The intensity of staining of these four islet hormones in the islets of the RIP-G Tg was not apparently different from those of nontransgenic littermates. The ratio of the β cell area to whole pancreas was not changed significantly

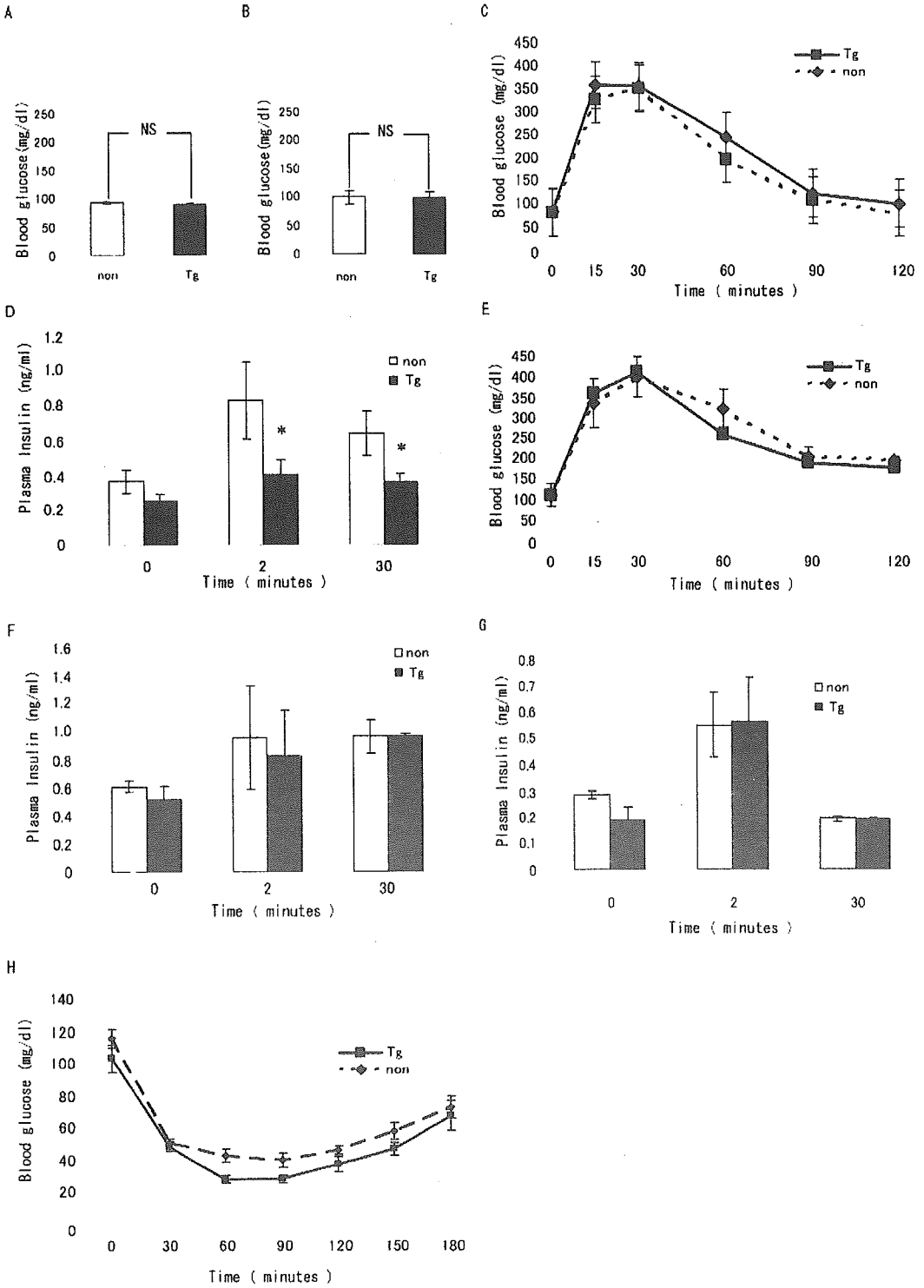

FIG. 4. *A* and *B*, blood glucose levels after overnight fast in RIP-G Tg (*A*) and RGP-G Tg (*B*) (*Tg*) and their nontransgenic littermates (*non*). *C* and *E*, intraperitoneal (*IP*) glucose tolerance test (1.5 g/kg) in RIP-G Tg (*C*) and RGP-G Tg (*E*) (*Tg*) and their nontransgenic littermates (*non*). *D* and *F*, plasma insulin concentration after intraperitoneal glucose (3g/kg) injection in RIP-G Tg (*D*) and RGP-G Tg (*F*) (*Tg*) and their nontransgenic littermates (*non*). *G*, plasma insulin concentration after intraperitoneal arginine (0.25g/kg) injection in RIP-G Tg (*Tg*) and their nontransgenic littermates (*non*). *H*, insulin (2.0 units/kg) tolerance test in RIP-G Tg (*Tg*) and their nontransgenic littermates (*non*). Values are represented as mean ± S.E. *, $p < 0.05$ compared with nontransgenic littermates.

(Fig. 5*I*). We also studied the tissue sections of RGP-G Tg and found no significant differences (Fig. 5, *E–H*, and *J*).

Expression of Insulin mRNA and Insulin Content—Because RIP-G Tg showed suppression of insulin secretion, we examined pancreatic mRNA expression and peptide content of insulin in RIP-G Tg and their nontransgenic littermates by Northern blot analysis and RIA. The insulin mRNA in RIP-G Tg did not differ from those of their nontransgenic littermates (Fig. 6, *A* and *B*). No significant differences of insulin contents were observed between RIP-G Tg and their nontransgenic littermates (Fig. 6*C*).

PDX-1 and GLUT2 Immunoreactivity—We examined the immunoreactivity of PDX-1 and GLUT2 in RIP-G Tg. The staining intensities of PDX-1 and GLUT2 in the RIP-G Tg (Fig. 7, *A*

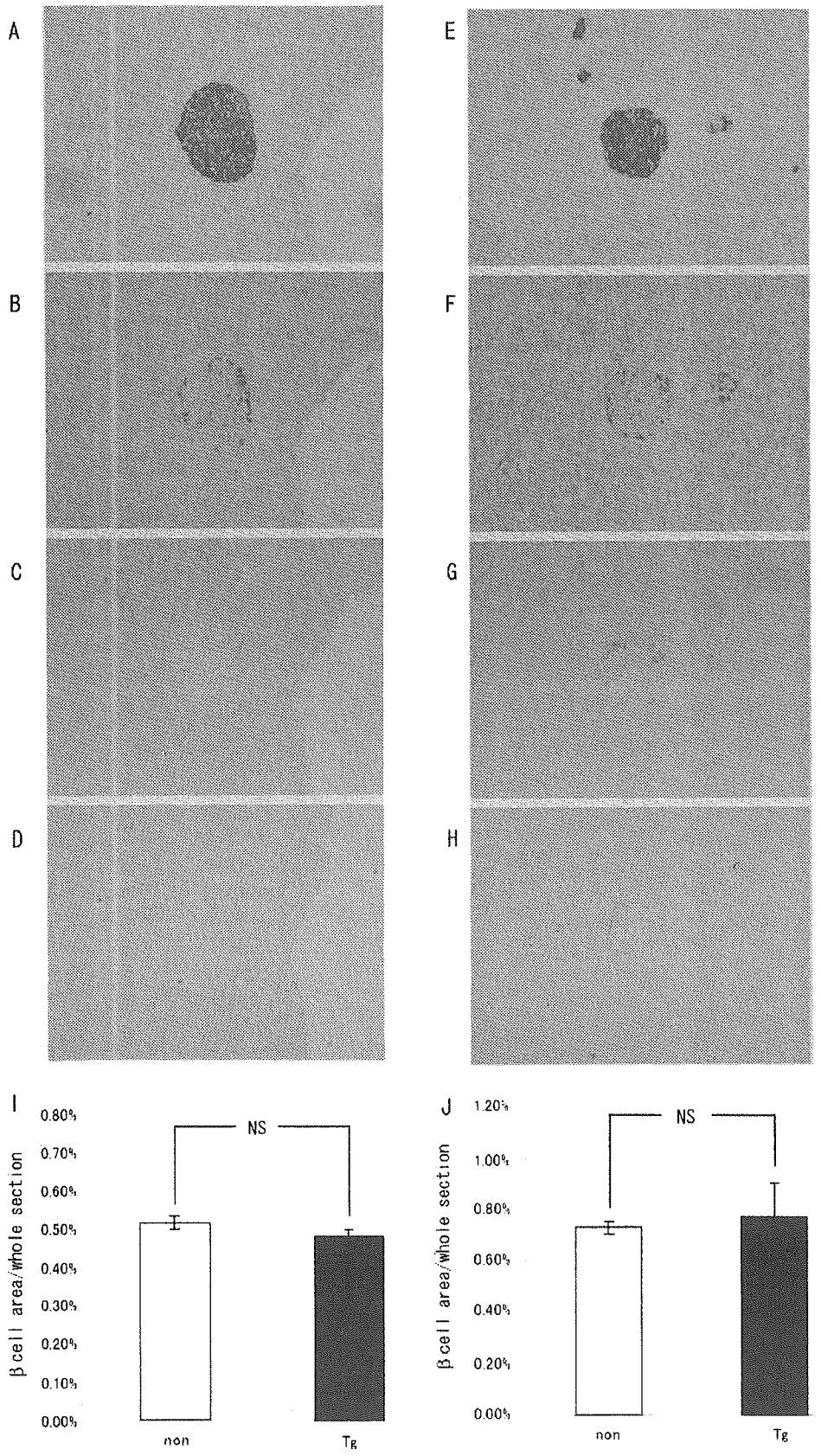

FIG. 5. **Islet morphology and β cell area in RIP-G Tg (*A–D*) and RGP-G Tg (*E–H*).** The sections were stained with anti-insulin (*A* and *E*), anti-glucagon (*B* and *F*), anti-somatostatin (*C* and *G*), and anti-PP antiserum (*D* and *H*). *I* and *J*, the ratio of β cell area to that of whole section in RIP-G Tg (*I*) and RGP-G Tg (*J*). *non*, nontransgenic littermates; *Tg*, RIP-G Tg; *NS*, not significant.

and *C*) were not apparently different from those in the nontransgenic littermates (Fig. 7, *B* and *D*).

Expression of GHS-R mRNA—To rule out possible down-regulation of GHS-R due to chronic exposure to high level ghrelin, we measured the expression level of GHS-R mRNA in pancreas and pituitary by real-time quantitative RT-PCR.

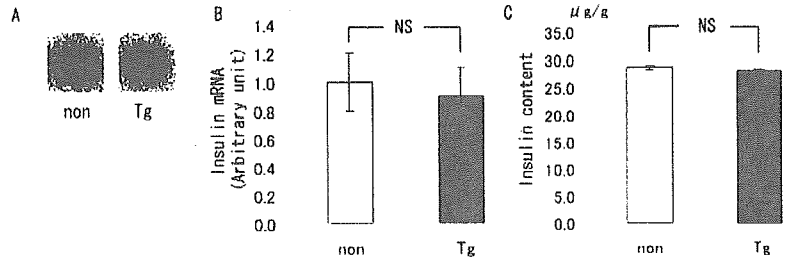

FIG. 6. **mRNA level and peptide content of insulin in RIP-G Tg (*Tg*) and their nontransgenic littermates (*non*) pancreas.** *A*, representative blot of Northern blot analysis of insulin; *B*, insulin mRNA levels; *C*, insulin peptide contents. *NS*, not significant.

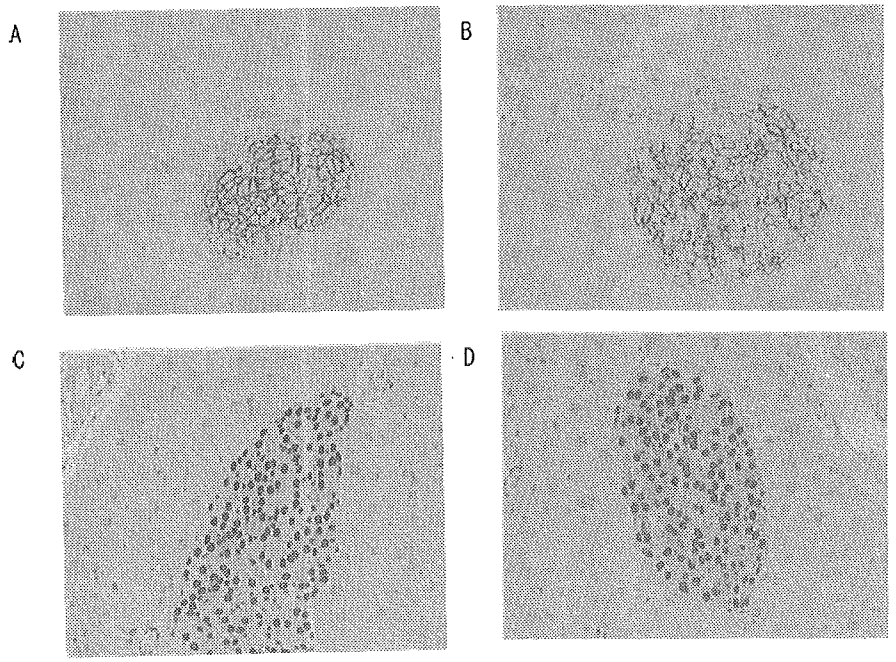

FIG. 7. *A* and *B*, immunoreactivity of Glut-2 in the islet of RIP-G Tg (*A*) and nontransgenic littermates (*B*). *C* and *D*, immunoreactivity of PDX-1 in the islet of RIP-G Tg (*C*) and nontransgenic littermates (*D*).

There were no significant differences in GHS-R mRNA levels between RIP-G Tg and their nontransgenic littermates either in pancreas (Fig. 8*A*) or in pituitary (Fig. 8*B*).

Batch Incubation of Islets—The insulin secretion from isolated islet of RIP-G Tg by batch incubation was indistinguishable from that of nontransgenic littermates, in 3.3 or 8.7 or 16.7 mM glucose conditions (Fig. 9).

Lipid Metabolism—Plasma total cholesterol level of RIP-G Tg tended to be lower than those of nontransgenic littermates, but it did not reach statistical significance (total cholesterol: 85.4 ± 6.9 *versus* 79.4 ± 7.5 mg/dl, $n = 6$, NS). The plasma triglyceride level of RIP-G Tg tended to be lower than that of nontransgenic littermates, but it did not reach statistical significance (154.5 ± 11.0 *versus* 136.9 ± 10.3 mg/dl, $n = 6$, NS). Free fatty acid level and HDL-cholesterol level of RIP-G Tg were not significantly different from those of nontransgenic littermates (free fatty acid; 0.44 ± 0.05 *versus* 0.48 ± 0.07 mEq/liter, $n = 6$, NS, HDL-cholesterol; 46.1 ± 2.3 *versus* 44.9 ± 3.4 mg/dl, $n = 6$, NS).

DISCUSSION

In wild-type mice, no ghrelin-like immunoreactivity was detected in most of the islets. C-terminal ghrelin-like immunoreactivity was observed in the periphery of minor proportion of islets of wild type mice, which is consistent with a previous report (24). By the serial section analysis, most of the ghrelin-producing cells also showed glucagon-like immunoreactivity. These findings indicate that ghrelin was expressed in minor proportion of mouse pancreatic α cells. Expression of ghrelin was not detected in pancreatic β cells of wild type mice.

In the present study we developed RIP-G Tg, in which pancreatic ghrelin concentration measured by C-RIA was ~1000 times higher than that of nontransgenic littermates. By immunohistochemistry using anti-C-terminal ghrelin [13–28] antiserum we detected C-terminal ghrelin-like immunoreactivity in almost the whole area of islets. Therefore, because ghrelin was not detected in β cells of control mice by immunohistochemistry, ghrelin transgene driven by RIP was considered to be expressed in β cells.

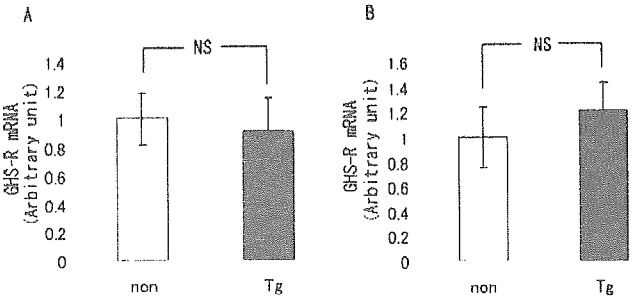

FIG. 8. **mRNA level of GHS-R determined by quantitative RT-PCR in pancreas (*A*) and pituitary (*B*) of RIP-G Tg (*Tg*) and their nontransgenic littermates (*non*).** *NS*, not significant.

We also found about 3 times higher expression level of ghrelin mRNA in the brain of RIP-G Tg compared with that of nontransgenic littermates, which could not be detected by immunohistochemistry. Although a small amount of ghrelin has been reported to be expressed in brain, which can be detected by immunohistochemistry only after colchicine treatment (1), there have been controversies as to whether this small amount of ghrelin in the brain has a biological role. Because the food intake of RIP-G Tg was not different from that of nontransgenic littermates, the ghrelin produced by transgene in the brain seems not to show bioactive effect of *n*-octanoylated ghrelin.

By immunohistochemistry using anti-ghrelin [1–11] anti-

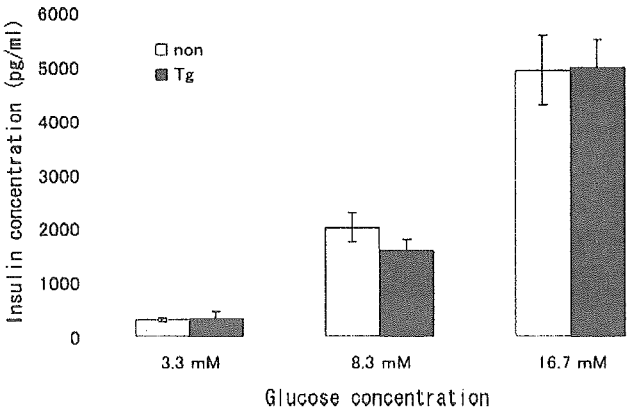

FIG. 9. **Batch incubation study of isolated islets of RIP-G Tg (*Tg*) and their nontransgenic littermates (*non*).**

serum that recognizes the *n*-octanoylated portion of ghrelin, ghrelin-like immunoreactivity was also demonstrated in nearly whole area of islets of RIP-G Tg, indicating the production of *n*-octanoylated ghrelin in β cells. This finding indicates that the mechanism of acylation may exist not only in pancreatic α cells but also in β cells. This is reasonable, because α and β cells are pancreatic endocrine cells derived from common precursor cells (40). Because the N-RIA/C-RIA ratio of the pancreatic tissue ghrelin concentration of RIP-G Tg was much lower than that of the stomach (0.0053% *versus* 11.67%, $p < 0.01$), the ability of acylation in β cell might be lower than that of in ghrelin-producing cell in the stomach (X/A-like cell). It is possible that exocrine pancreatic enzymes might interfere with the results, although these were inactivated by boiling before extraction. The other possibility is that because of the formalin fixation of ghrelin in the tissue section the epitope recognized by immunohistochemistry using anti-ghrelin [1–11] antiserum might not be exactly the same as that recognized by N-RIA or enzyme-linked immunosorbent assay. Because the amount of *n*-octanoylated ghrelin was so little that it could not be detected by RIA if any, we considered that the phenotype of these transgenic mice is due to the effect of desacyl ghrelin. Desacyl ghrelin has been shown not to activate GHS-R (39). There have been several reports saying that desacyl ghrelin has biological activities, such as promoting adipogenesis (41), inhibition of cell proliferation, inhibition of apoptosis (42), and counteracting the effect of *n*-octanoylated ghrelin (35).

We showed here that the ghrelin level in portal vein is significantly higher than that in retroorbital vein in wild type mouse. Ghrelin has been reported to be mainly synthesized in stomach and intestine. The step-up of plasma ghrelin level in gastric vein has been reported previously (43), but there has been no report showing the step-up of plasma ghrelin level in portal vein as compared with that in systemic circulation. The present study is the first report of the step-up of plasma ghrelin levels in portal vein. Moreover, the step-up of desacyl ghrelin in RIP-G Tg was much higher than that in control littermates, indicating overproduction of desacyl ghrelin by transgene in the pancreas.

The body weight, percent body fat, and food consumption of RIP-G Tg were not significantly different from those of nontransgenic littermates. Recently, we and Asakawa *et al.* have reported the studies of β-actin promoter ghrelin transgenic mouse (44, 45), in which plasma desacyl ghrelin levels were 30 and 50 times higher than those of their nontransgenic littermates. These transgenic mice were reported to show small phenotype, although some discrepancy of interpretation regarding on etiology exists. Asakawa *et al.* reported that the triglyceride level of β-actin promoter ghrelin transgenic mouse was lower, but that cholesterol level and free fatty acid level were not changed compared with their nontransgenic littermates. The triglyceride levels of our RIP-G Tg only showed lower tendency compared with that of nontransgenic littermates. The lack of small phenotype and milder phenotype of lipid metabolism in RIP-G Tg may result from the fact that plasma desacyl ghrelin level of RIP-G Tg was only 3.4 times higher than those of nontransgenic littermates.

The tissue sections of the pancreas of these transgenic mice showed no apparent disarrangement in the islet architecture and in β cell mass. There have been several reports on the transgenic mice overexpressing humoral factors in the β cells, such as parathyroid hormone-related peptide, hepatocyte growth factor, and insulin-like growth factor-I (46–49). Some of these transgenic mice showed islet hypertrophy or disarrangement of the endocrine cells in the islet (46–49). Our observation showed that desacyl ghrelin might have no apparent effects on the islet architecture and β cell mass.

In the present study plasma insulin levels after the 3.0 g/kg glucose injection were significantly lower in RIP-G Tg than those in nontransgenic littermates, although there was no significant difference in plasma insulin levels between RIP-G Tg and nontransgenic littermates on the fasting state. To rule out the decreased production of insulin caused by exogenous insulin promoter, we measured insulin mRNA level and content in the pancreata of our transgenic mice. The insulin mRNA level and content from the transgenic mice were not significantly different from those from nontransgenic littermates. Therefore, the insulin production might not be disturbed in these mice either in transcriptional or translational levels. The immunoreactivity of PDX-1, which is the master regulator of the pancreas development and essential for insulin transcription, in RIP-G Tg β cell was not different from that in β cells of nontransgenic littermates. These results suggest that the suppression of glucose-stimulated insulin secretion in RIP-G Tg might not be due to the transcriptional dysregulation of insulin caused by injection of exogenous insulin promoter.

RIP-G Tg did not show decreased-insulin secretion in response to arginine. Arginine is known to stimulate insulin secretion by the mechanisms that are different from those used by glucose, although the detail remains controversial (50, 51). However, it seems certain that arginine somehow evoked Ca^{2+} influx into the β cell, and that leads to the exocytosis of insulin-containing vesicles (52, 53). So at least, the decreased insulin secretion in RIP-G Tg might not be due to disorders in exocytosis process. Egido (28) reported that ghrelin inhibits insulin secretion from rat pancreas in response to arginine *in vitro*, however, there has been no report on the effect of desacyl ghrelin on arginine-induced insulin secretion.

The immunoreactivity of GLUT2, glucose transporter in the pancreatic β cell, in RIP-G Tg β cells, was indistinguishable from that in the β cells of nontransgenic littermates. Although immunohistochemistry is not so suitable for quantitative analysis, at least no apparent decreased expression or disposition of GLUT2 in RIP-G Tg β cell exists. Chronic exposure to the high level of desacyl ghrelin may not influence on GLUT2 expression.

We performed a batch incubation study of RIP-G Tg islet. The insulin secretion from isolated islets of RIP-G Tg was indistinguishable from that of nontransgenic littermates. This finding indicates that insulin secretion was not affected by overexpression of ghrelin transgene *in vitro* but was affected *in vivo*. The different observations *in vitro* and *in vivo* may be explained by dilution of ghrelin produced by transgene with the incubation buffer. Alternatively, suppression of insulin secretion of RIP-G Tg was not due to the effect of desacyl ghrelin on

insulin secretion from β cell but on insulin sensitivity. Recently Gauna *et al.* (55) reported that co-administration of desacyl ghrelin and active ghrelin improves insulin sensitivity in humans (54) and that desacyl ghrelin suppress glucose output from liver. Although an insulin tolerance test did not show a statistically significant difference in blood glucose levels between RIP-G Tg and their nontransgenic littermates, there was a tendency for lower blood glucose levels of RIP-G Tg. Moreover, plasma triglyceride levels of RIP-G Tg showed lower tendency. Taken together, these results may indicate that desacyl ghrelin may improve insulin sensitivity of RIP-G Tg. The suppression of insulin secretion of RIP-G Tg is likely due to the effect of desacyl ghrelin on insulin sensitivity.

To explore if chronic exposure to high level desacyl ghrelin may influence the expression level of GHS-R, we investigated the mRNA level of GHS-R in the pancreas and pituitary of RIP-G Tg. No significant differences were found in GHS-R mRNA levels in pancreas or in pituitary between RIP-G Tg and their nontransgenic littermates. These findings indicate that chronic exposure to high level desacyl ghrelin might not influence the GHS-R mRNA expression level.

We also developed RGP-G Tg. The pancreatic tissue ghrelin concentrations determined by C-RIA of RGP-G Tg were about 50 times higher than those of their nontransgenic littermates, indicating that ghrelin was overexpressed in RGP-G Tg. However, there was no obvious phenotype regarding insulin secretion and pancreatic morphology. Considering the observation that portal ghrelin levels were not elevated in RGP-G Tg compared with those in their nontransgenic littermates, the amount of secreted ghrelin from α cell may not outstrip the amount from stomach.

In summary we developed RIP-G Tg, in which pancreatic desacyl ghrelin content was ~1,000 times higher than that in control littermates. We detected *n*-octanoylated ghrelin-like immunoreactivity in pancreatic β cells by immunohistochemistry, indicating that the mechanism of acylation may exist not only in pancreatic α cells but also in β cells. The glucose-stimulated insulin secretion of RIP-G Tg was decreased. There were no abnormalities with the arginine-induced insulin secretion, pancreatic histology, pancreatic insulin mRNA levels, and insulin content in the RIP-G Tg. The absence of insulin suppression in the islet batch incubation study, lower tendency of blood glucose levels in insulin tolerance test, and lower tendency of plasma triglyceride level may indicate that the suppression of insulin secretion of RIP-G Tg is likely due to the effect of desacyl ghrelin on insulin sensitivity. Although we also developed RGP-G Tg with a 50-fold increase of pancreatic desacyl ghrelin content, we did not find obvious phenotype regarding insulin secretion and pancreatic morphology. The present study raises the possibility that desacyl ghrelin may have an influence on glucose metabolism.

REFERENCES

1. Kojima, M., Hosoda, H., Date, Y., Nakazato, M., Matsuo, H., and Kangawa, K. (1999) *Nature* **402,** 656–660
2. Date, Y., Kojima, M., Hosoda, H., Sawaguchi, A., Mondal, M. S., Suganuma, T., Matsukura, S., Kangawa, K., and Nakazato, M. (2000) *Endocrinology* **141,** 4255–4261
3. Gualillo, O., Caminos, J., Blanco, M., Garcia-Caballero, T., Kojima, M., Kangawa, K., Dieguez, C., and Casanueva, F. (2001) *Endocrinology* **142,** 788–794
4. Mori, K., Yoshimoto, A., Takaya, K., Hosoda, K., Ariyasu, H., Yahata, K., Mukoyama, M., Sugawara, A., Hosoda, H., Kojima, M., Kangawa, K., and Nakao, K. (2000) *FEBS Lett.* **486,** 213–216
5. Korbonits, M., Kojima, M., Kangawa, K., and Grossman, A. B. (2001) *Endocrine* **14,** 101–104
6. Tena-Sempere, M., Barreiro, M. L., Gonzalez, L. C., Gaytan, F., Zhang, F. P., Caminos, J. E., Pinilla, L., Casanueva, F. F., Dieguez, C., and Aguilar, E. (2002) *Endocrinology* **143,** 717–725
7. Asakawa, A., Inui, A., Kaga, T., Yuzuriha, H., Nagata, T., Fujimiya, M., Katsuura, G., Makino, S., Fujino, M. A., and Kasuga, M. (2001) *Neuroendocrinology* **74,** 143–147
8. Masuda, Y., Tanaka, T., Inomata, N., Ohnuma, N., Tanaka, S., Itoh, Z., Hosoda, H., Kojima, M., and Kangawa, K. (2000) *Biochem. Biophys. Res. Commun.* **276,** 905–908
9. Shintani, M., Ogawa, Y., Ebihara, K., Aizawa-Abe, M., Miyanaga, F., Takaya, K., Hayashi, T., Inoue, G., Hosoda, K., Kojima, M., Kangawa, K., and Nakao, K. (2001) *Diabetes* **50,** 227–232
10. Seoane, L. M., Tovar, S., Baldelli, R., Arvat, E., Ghigo, E., Casanueva, F. F., and Dieguez, C. (2000) *Eur. J. Endocrinol.* **143,** R7–R9
11. Takaya, K., Ariyasu, H., Kanamoto, N., Iwakura, H., Yoshimoto, A., Harada, M., Mori, K., Komatsu, Y., Usui, T., Shimatsu, A., Ogawa, Y., Hosoda, K., Akamizu, T., Kojima, M., Kangawa, K., and Nakao, K. (2000) *J. Clin. Endocrinol. Metab.* **85,** 4908–4911
12. Arvat, E., Di Vito, L., Broglio, F., Papotti, M., Muccioli, G., Dieguez, C., Casanueva, F. F., Deghenghi, R., Camanni, F., and Ghigo, E. (2000) *J. Endocrinol. Invest.* **23,** 493–495
13. Date, Y., Murakami, N., Kojima, M., Kuroiwa, T., Matsukura, S., Kangawa, K., and Nakazato, M. (2000) *Biochem. Biophys. Res. Commun.* **275,** 477–480
14. Date, Y., Nakazato, M., Murakami, N., Kojima, M., Kangawa, K., and Matsukura, S. (2001) *Biochem. Biophys. Res. Commun.* **280,** 904–907
15. Nagaya, N., Uematsu, M., Kojima, M., Ikeda, Y., Yoshihara, F., Shimizu, W., Hosoda, H., Hirota, Y., Ishida, H., Mori, H., and Kangawa, K. (2001) *Circulation* **104,** 1430–1435
16. Tschop, M., Smiley, D. L., and Heiman, M. L. (2000) *Nature* **407,** 908–913
17. Wren, A. M., Small, C. J., Ward, H. L., Murphy, K. G., Dakin, C. L., Taheri, S., Kennedy, A. R., Roberts, G. H., Morgan, D. G., Ghatei, M. A., and Bloom, S. R. (2000) *Endocrinology* **141,** 4325–4328
18. Nakazato, M., Murakami, N., Date, Y., Kojima, M., Matsuo, H., Kangawa, K., and Matsukura, S. (2001) *Nature* **409,** 194–198
19. Inui, A. (2001) *Nat. Rev. Neurosci.* **2,** 551–560
20. Date, Y., Nakazato, M., Hashiguchi, S., Dezaki, K., Mondal, M. S., Hosoda, H., Kojima, M., Kangawa, K., Arima, T., Matsuo, H., Yada, T., and Matsukura, S. (2002) *Diabetes* **51,** 124–129
21. Volante, M., Allia, E., Gugliotta, P., Funaro, A., Broglio, F., Deghenghi, R., Muccioli, G., Ghigo, E., and Papotti, M. (2002) *J. Clin. Endocrinol. Metab.* **87,** 1300–1308
22. Wierup, N., Svensson, H., Mulder, H., and Sundler, F. (2002) *Regul. Pept.* **107,** 63–69
23. Wierup, N., Yang, S., McEvilly, R. J., Mulder, H., and Sundler, F. (2004) *J. Histochem. Cytochem.* **52,** 301–310
24. Prado, C. L., Pugh-Bernard, A. E., Elghazi, L., Sosa-Pineda, B., and Sussel, L. (2004) *Proc. Natl. Acad. Sci. U. S. A.* **101,** 2924–2929
25. Sun, Y., Ahmed, S., and Smith, R. G. (2003) *Mol. Cell. Biol.* **23,** 7973–7981
26. Wortley, K. E., Anderson, K. D., Garcia, K., Murray, J. D., Malinova, L., Liu, R., Moncrieffe, M., Thabet, K., Cox, H. J., Yancopoulos, G. D., Wiegand, S. J., and Sleeman, M. W. (2004) *Proc. Natl. Acad. Sci. U. S. A.* **101,** 8227–8232
27. Broglio, F., Arvat, E., Benso, A., Gottero, C., Muccioli, G., Papotti, M., van der Lely, A. J., Deghenghi, R., and Ghigo, E. (2001) *J. Clin. Endocrinol. Metab.* **86,** 5083–5086
28. Egido, E. M., Rodriguez-Gallardo, J., Silvestre, R. A., and Marco, J. (2002) *Eur. J. Endocrinol.* **146,** 241–244
29. Reimer, M. K., Pacini, G., and Ahren, B. (2003) *Endocrinology* **144,** 916–921
30. Broglio, F., Gottero, C., Benso, A., Prodam, F., Destefanis, S., Gauna, C., Maccario, M., Deghenghi, R., van der Lely, A. J., and Ghigo, E. (2003) *J. Clin. Endocrinol. Metab.* **88,** 4268–4272
31. Adeghate, E., and Ponery, A. S. (2002) *J. Neuroendocrinol.* **14,** 555–560
32. Lee, H. M., Wang, G., Englander, E. W., Kojima, M., and Greeley, G. H., Jr. (2002) *Endocrinology* **143,** 185–190
33. Salehi, A., Dornonville De La Cour, C., Hakanson, R., and Lundquist, I. (2004) *Regul. Pept.* **118,** 143–150
34. Broglio, F., Benso, A., Gottero, C., Prodam, F., Gauna, C., Filtri, L., Arvat, E., van der Lely, A. J., Deghenghi, R., and Ghigo, E. (2003) *J. Endocrinol. Invest* **26,** 192–196
35. Broglio, F., Gottero, C., Prodam, F., Gauna, C., Muccioli, G., Papotti, M., Abribat, T., Van Der Lely, A. J., and Ghigo, E. (2004) *J. Clin. Endocrinol. Metab.* **89,** 3062–3065
36. Iwakura, H., Hosoda, K., Doi, R., Komoto, I., Nishimura, H., Son, C., Fujikura, J., Tomita, T., Takaya, K., Ogawa, Y., Hayashi, T., Inoue, G., Akamizu, T., Hosoda, H., Kojima, M., Kangawa, K., Imamura, M., and Nakao, K. (2002) *J. Clin. Endocrinol. Metab.* **87,** 4885–4888
37. Guz, Y., Montminy, M. R., Stein, R., Leonard, J., Gamer, L. W., Wright, C. V., and Teitelman, G. (1995) *Development* **121,** 11–18
38. Thorens, B., Sarkar, H. K., Kaback, H. R., and Lodish, H. F. (1988) *Cell* **55,** 281–290
39. Hosoda, H., Kojima, M., Matsuo, H., and Kangawa, K. (2000) *Biochem. Biophys. Res. Commun.* **279,** 909–913
40. Herrera, P. L., Nepote, V., and Delacour, A. (2002) *Endocrine* **19,** 267–278
41. Thompson, N. M., Gill, D. A., Davies, R., Loveridge, N., Houston, P. A., Robinson, I. C., and Wells, T. (2004) *Endocrinology* **145,** 234–242
42. Baldanzi, G., Filigheddu, N., Cutrupi, S., Catapano, F., Bonissoni, S., Fubini, A., Malan, D., Baj, G., Granata, R., Broglio, F., Papotti, M., Surico, N., Bussolino, F., Isgaard, J., Deghenghi, R., Sinigaglia, F., Prat, M., Muccioli, G., Ghigo, E., and Graziani, A. (2002) *J. Cell Biol.* **159,** 1029–1037
43. Murakami, N., Hayashida, T., Kuroiwa, T., Nakahara, K., Ida, T., Mondal, M. S., Nakazato, M., Kojima, M., and Kangawa, K. (2002) *J. Endocrinol.* **174,** 283–288
44. Ariyasu, H., Takaya, K., Iwakura, H., Hosoda, H., Akamizu, T., Arai, Y., Kangawa, K., and Nakao, K. (2005) *Endocrinology* **146,** 355–364
45. Asakawa, A., Inui, A., Fujimiya, M., Sakamaki, R., Shinfuku, N., Ueta, Y., Meguid, M. M., and Kasuga, M. (2005) *Gut* **54,** 18–24
46. Garcia-Ocana, A., Takane, K. K., Syed, M. A., Philbrick, W. M., Vasavada,

R. C., and Stewart, A. F. (2000) *J. Biol. Chem.* **275,** 1226–1232
47. Porter, S. E., Sorenson, R. L., Dann, P., Garcia-Ocana, A., Stewart, A. F., and Vasavada, R. C. (1998) *Endocrinology* **139,** 3743–3751
48. Dheen, S. T., Rajkumar, K., and Murphy, L. J. (1997) *J. Endocrinol.* **155,** 551–558
49. Petrik, J., Pell, J. M., Arany, E., McDonald, T. J., Dean, W. L., Reik, W., and Hill, D. J. (1999) *Endocrinology* **140,** 2353–2363
50. Smith, P. A., Sakura, H., Coles, B., Gummerson, N., Proks, P., and Ashcroft, F. M. (1997) *J. Physiol.* **499,** 625–635
51. Schmidt, H. H., Warner, T. D., Ishii, K., Sheng, H., and Murad, F. (1992) *Science* **255,** 721–723
52. Gilon, P., and Henquin, J. C. (1992) *J. Biol. Chem.* **267,** 20713–20720
53. Weinhaus, A. J., Poronnik, P., Cook, D. I., and Tuch, B. E. (1995) *Diabetes* **44,** 118–124
54. Gauna, C., Meyler, F. M., Janssen, J. A., Delhanty, P. J., Abribat, T., van Koetsveld, P., Hofland, L. J., Broglio, F., Ghigo, E., and van der Lely, A. J. (2004) *J. Clin. Endocrinol. Metab.* **89,** 5035–5042
55. Gauna, C., Delhanty, P. J., Hofland, L. J., Janssen, J. A., Broglio, F., Ross, R. J., Ghigo, E., and van der Lely, A. J. (2005) *J. Clin. Endocrinol. Metab.* **90,** 1055–1060

Hypertension
JOURNAL OF THE AMERICAN HEART ASSOCIATION

Role of Natriuretic Peptide Receptor Guanylyl Cyclase-A in Myocardial Infarction Evaluated Using Genetically Engineered Mice

Michio Nakanishi, Yoshihiko Saito, Ichiro Kishimoto, Masaki Harada, Koichiro Kuwahara, Nobuki Takahashi, Rika Kawakami, Yasuaki Nakagawa, Keiji Tanimoto, Shinji Yasuno, Satoru Usami, Yuhao Li, Yuichiro Adachi, Akiyoshi Fukamizu, David L. Garbers and Kazuwa Nakao

Hypertension 2005;46;441-447; originally published online Jul 5, 2005;
DOI: 10.1161/01.HYP.0000173420.31354.ef
Hypertension is published by the American Heart Association. 7272 Greenville Avenue, Dallas, TX 72514
 Print ISSN: 0194-911X. Online ISSN: 1524-4563

Role of Natriuretic Peptide Receptor Guanylyl Cyclase-A in Myocardial Infarction Evaluated Using Genetically Engineered Mice

Michio Nakanishi, Yoshihiko Saito, Ichiro Kishimoto, Masaki Harada, Koichiro Kuwahara, Nobuki Takahashi, Rika Kawakami, Yasuaki Nakagawa, Keiji Tanimoto, Shinji Yasuno, Satoru Usami, Yuhao Li, Yuichiro Adachi, Akiyoshi Fukamizu, David L. Garbers, Kazuwa Nakao

Abstract—Although plasma levels of atrial natriuretic peptide (ANP) and brain natriuretic peptide (BNP) are elevated early after myocardial infarction (MI), the significance is not fully understood. We therefore investigated the function of natriuretic peptides after induction of MI in knockout (KO) mice lacking the natriuretic peptide receptor guanylyl cyclase-A, the receptor for ANP and BNP. KO and wild-type (WT) mice were subjected to left coronary artery ligation and then followed up for 4 weeks. Irrespective of genotype, almost all deaths occurred within 1 week after induction of MI. KO mice showed significantly higher mortality because of a higher incidence of acute heart failure, which was associated with diminished water and sodium excretion and with higher cardiac levels of mRNAs encoding ANP, BNP, transforming growth factor-β1, and type I collagen. By 4 weeks after infarction, left ventricular remodeling, including myocardial hypertrophy and fibrosis, and impairment of left ventricular systolic function were significantly more severe in KO than WT mice. Notably, the enhanced myocardial fibrosis seen in KO mice was virtually absent in infarcted double-KO mice, lacking guanylyl cyclase-A and angiotensin II type 1a receptors, although there was no improvement in survival and no attenuation of cardiac hypertrophy. Thus, guanylyl cyclase-A activation by endogenous cardiac natriuretic peptides protects against acute heart failure and attenuates chronic cardiac remodeling after MI. These beneficial effects are mediated partly through inhibition of the renin-angiotensin system (RAS), although RAS-independent protective actions of guanylyl cyclase-A are also suggested. (***Hypertension*. 2005;46:441-447.**)

Key Words: receptors, angiotensin ■ coronary artery disease ■ hypertrophy ■ remodeling

Early reperfusion therapy and other recent advances in the treatment of acute myocardial infarction (MI) have substantially reduced mortality and cardiovascular morbidity among MI patients. However, the fact that acute heart failure and chronic left ventricular (LV) remodeling continue to be major determinants of clinical outcome after MI highlights the need for a better understanding of the pathophysiological mechanisms involved in those processes. In that regard, accumulating clinical and experimental evidence indicates that inhibition of the renin-angiotensin system (RAS) and the sympathetic nervous system improves postinfarct survival and mitigates LV remodeling and dysfunction.[1–4]

Atrial natriuretic peptide (ANP) and brain natriuretic peptide (BNP) are produced mainly in the atrial and ventricular myocardium, respectively, in response to volume expansion and pressure overload and counteract the effects of the sympathetic nervous system and RAS by promoting diuresis, natriuresis, and vasodilatation. The actions of both peptides are mediated via the natriuretic peptide receptor guanylyl cyclase-A (GC-A), which is expressed in a variety of tissues, including kidneys, blood vessels, adrenal glands, and heart.[5] Plasma levels of natriuretic peptides are elevated in congestive heart failure (CHF) and are frequently used to aid diagnosis of CHF, to assess prognosis, and to tailor therapy.[6–9] In addition, exogenous administration of recombinant natriuretic peptides is now being used therapeutically to treat decompensated CHF.[10]

Plasma natriuretic peptide levels are also elevated early after MI;[11] in particular, the level of BNP has been shown to be a good predictor of LV systolic function and a prognostic indicator of long-term survival.[12] Although in a previous study, we suggested a role for GC-A in myocardial reperfusion injury and inflammation after ischemia-reperfusion,[13] it remains unclear whether activation of the GC-A pathway by endogenous natriuretic peptides has a significant effect on survival or LV remodeling after MI. Therefore, to better

Received November 21, 2004; first decision December 9, 2004; revision accepted April 2, 2005.

From the Department of Medicine and Clinical Science, Kyoto University Graduate School of Medicine (M.N., I.K., M.H., K.K., N.T., R.K., Y.N., K.T., S.Y., S.U., Y.L., Y.A., K.N.), Japan; the First Department of Internal Medicine, Nara Medical University, Japan (Y.S.); the Center for Tsukuba Advanced Research Alliance, Institute of Applied Biochemistry, University of Tsukuba, Ibaraki, Japan (A.F.); and the Howard Hughes Medical Institute and Department of Pharmacology, University of Texas, Southwestern Medical Center at Dallas (D.L.G.).

Correspondence to Ichiro Kishimoto, MD, PhD, Department of Biochemistry, National Cardiovascular Center, Research Institute, 5-7-1 Fujishiro-dai, Suita City, Osaka 565-8565, Japan. E-mail kishimot@ri.ncvc.go.jp

Hypertension **is available at http://www.hypertensionaha.org** **DOI: 10.1161/01.HYP.0000173420.31354.ef**

understand the function and significance of the increased natriuretic peptide levels seen after MI, we induced MI by occluding the left coronary artery (LCA) in GC-A knockout (KO) mice and their wild-type (WT) littermates and examined survival, LV structure, LV function, and cardiac gene expression.

Materials and Methods

Experimental Model

All experimental procedures were performed according to Kyoto University standards for animal care. Homozygous GC-A KO mice and their WT littermates were produced from crossing heterozygous mice as described previously,[14] after which male mice were used for experimentation at 8 to 10 weeks of age.

Experimental MI

MI was produced by permanent ligation of the LCA, and sham-operated mice underwent the same operation except for the LCA ligation. Infarct size was calculated and expressed as the ratio of the infarcted circumference divided by total LV circumference, as described previously.[15]

Noninvasive Blood Pressure Measurements

Blood pressures and pulse rates were measured noninvasively in conscious mice using a computerized tail-cuff method (Softron Co, Ltd).

Urine Volume and Sodium Excretion

Animals were kept in individual metabolic cages from the day before surgery until 4 days after surgery. Urine was collected daily, and urine volume and sodium excretion were measured. Data were normalized to body weight (BW).

Cardiac Gene Expression

On day 3 after surgery, hearts were excised and the LVs were snap-frozen in liquid nitrogen. Total RNA was extracted from LVs, and expression of mRNAs was evaluated using quantitative RT-PCR analysis with gene-specific primers and probes in an ABI PRISM 7700 Sequence Detector (Applied Biosystems). Expression of the RNA in question was normalized to that of the corresponding GAPDH mRNA.

Echocardiography Examination

After anesthetizing mice by intraperitoneal administration of a mixture of ketamine (100 mg/kg) and xylazine (5 mg/kg), LV end-diastolic diameter (LVEDD), LV end-systolic diameter (LVESD), percent fractional shortening (%FS), and LV posterior wall (PW) thickness were calculated before (baseline) and 4 weeks after induction of MI using an echocardiographic system (Toshiba Power Vision 8000) equipped with a 12-MHz imaging transducer.

Histological Analysis

To determine the degree of collagen fiber accumulation, we randomly selected 20 fields in 3 separate sections of formalin-fixed ventricles and calculated the ratio of the van Gieson–stained fibrotic area to the total myocardial area using image analysis software (KS400 image system; Zeiss).

Double-KO Mice Lacking GC-A and Angiotensin II Type 1a Receptors

Double-KO (DKO) mice lacking GC-A and angiotensin II type 1a (AT1a) receptors were generated from heterozygous mice after crossing of a single GC-A KO mouse and an AT1a KO mice.[16]

TABLE 1. Baseline Characteristics and Causes of Death After MI

Variables	WT (n=37)	GC-A KO (n=33)
Baseline characteristics		
Age (weeks)	9.6±0.2	9.2±0.1
BW (g)	25.3±0.4	25.7±0.5
Systolic BP (mm Hg)	98.9±1.5	128.3±1.5*
PR (bpm)	569.9±13.9	553.6±10.4
Causes of death, n (%)		
Heart failure	2 (5.4%)	18 (54.5%)*
LV rupture	8 (21.6%)	5 (15.2%)
Unknown	1 (2.7%)	1 (3.0%)

BP indicates blood pressure; PR, pulse rate.
Values are mean±SEM; *$P<0.05$ vs WT mice.

Hydralazine Administration

The blood pressures of GC-A KO mice were reduced to a level comparable to those seen in WT mice by orally administering hydralazine (50 mg/L of drinking water). Hydralazine was started 1 week before MI and continued until death, 4 weeks after MI.

Statistical Analysis

All data are expressed as means±SEM. Analysis of survival after MI was performed using the Kaplan–Meier method with the log-rank test. Data were analyzed by 1-factor ANOVA. If a statistically significant effect was found, a post hoc Newman–Keuls test was performed to isolate the differences between groups. Values of $P<0.05$ were considered significant.

Results

Survival After MI

The baseline characteristics of the KO and WT genotypes are shown in Table 1. There were no differences with respect to age, BW, or pulse rate between the 2 groups, although blood pressure was significantly higher in KO mice, as reported previously.[14,17] Postoperative survival was monitored for 4 weeks (Figure 1). Irrespective of genotype, all deaths but 1 occurred within 1 week after induction of MI; 1 WT mouse

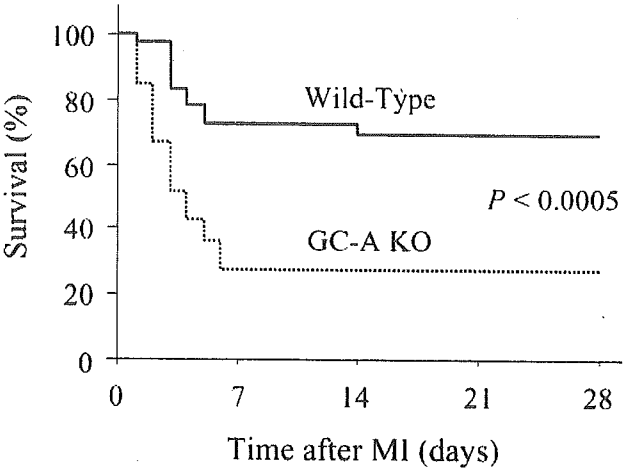

Figure 1. Kaplan–Meier analysis of survival after MI among WT (n=37) and GC-A KO mice (n=33). GC-A KO mice showed a significantly higher 4-week mortality rate than WT mice ($P<0.0005$).

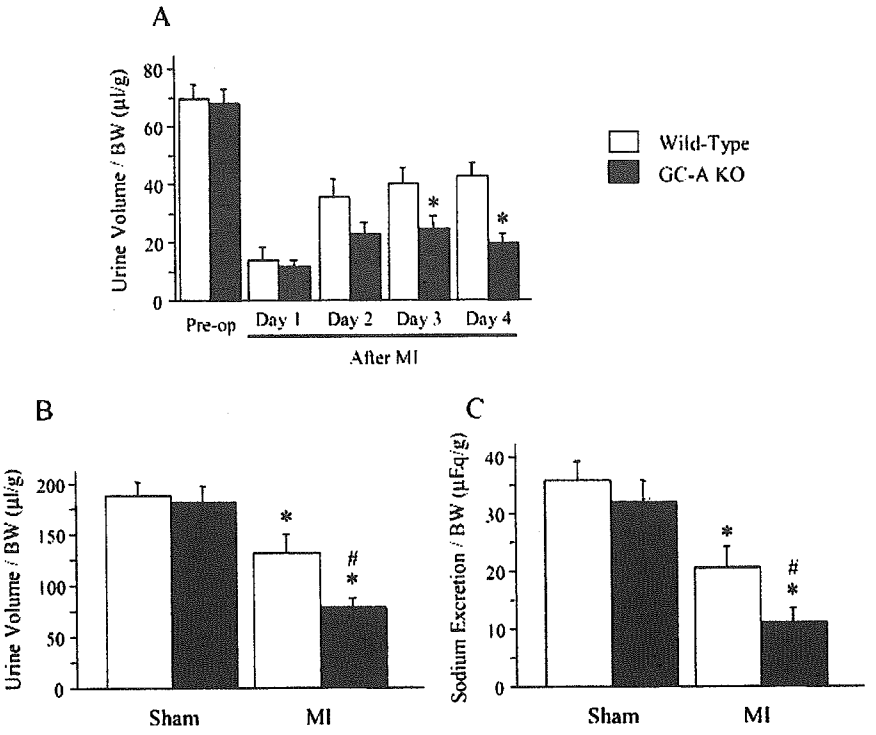

Figure 2. Diuretic and natriuretic responses before and after MI. A, Urine volumes were measured 1 day before (pre-op) and on days 1 through 4 after induction of MI and normalized to the corresponding BWs; *P<0.05 vs WT mice on each day. B and C, Total 4-day urine volume (B) and sodium excretion (C) were measured after induction of MI or sham operation and normalized to the corresponding BW. Values are means±SEM (n=12 for WT mice; n=16 for KO mice); *P<0.01 vs sham in each strain; #P<0.05 vs WT mice with MI.

died on day 14 after MI. Despite the fact that infarct sizes were similar in the 2 groups (KO 43.7±1.2% versus WT 46.8±1.8%), the survival rate was significantly (P<0.0005) lower among KO mice (27.3%; 9 of 33) than among WT mice (70.3%; 26 of 37).

Causes of Death

Based on postmortem findings, the causes of death were classified into 3 groups: heart failure, LV rupture, or unknown causes (Table 1). Heart failure was diagnosed from pulmonary congestion with increased lung weight, and LV rupture from the large amount of blood observed filling the chest cavity. The incidence of heart failure was significantly higher among KO mice than WT mice, although there were no significant differences between the 2 groups in the incidences of LV rupture or death by unknown causes.

Natriuretic and Diuretic Responses During Early Phase After MI

As shown in Figure 2A, there was no difference in urine volume between the 2 genotypes before surgery, and urine volume was markedly lower in both groups on day 1 after MI. Thereafter, volume increased gradually in both genotypes, but less so in KO mice. As a consequence, KO mice were producing significantly less urine than WT mice on days 3 and 4 after MI.

When we compared the renal responses of infarcted and sham-operated mice (Figure 2B and 2C), we found that the total 4-day urine volume and sodium excretion after the sham operation were similar for both genotypes. In contrast, over the course of 4 days after induction of MI, KO mice produced significantly less urine and excreted significantly less sodium than WT mice.

Cardiac Gene Expression During Early Phase After MI

On day 3 after sham operation, ventricular levels of ANP and BNP mRNA (Figure 3A and 3B) were higher in KO than WT hearts, probably because of basal LV hypertrophy in the former. In response to MI, both genotypes showed significant upregulation of ANP and BNP mRNA, but the postinfarction levels were still significantly higher in KO mice.

The cardiac expression of the mRNAs for transforming growth factor-β1 (TGF-β1) and type I collagen (Figure 3C and 3D) were similar in sham-operated WT and KO mice. Three days after MI, both genotypes showed significantly upregulated expression of TGF-β1 and type I collagen mRNA, but the postinfarction levels were significantly higher in KO than WT mice.

Echocardiographic Findings During Late Phase After MI

To evaluate chronic LV remodeling, echocardiographic examination of the infarcted mice was performed before (baseline) and 4 weeks after induction of MI (Table 2). Baseline measurements showed KO mice to have greater LVEDD, LVESD, and PW thickness than WT mice, but %FS was similar, as reported previously.[17] Four weeks after MI, both genotypes showed significant chamber enlargement and impaired LV contractility. Although no significant difference in the absolute increase in LVEDD was observed, the absolute decrease in %FS and the absolute increases in LVESD and PW thickness were significantly greater in KO than in WT mice.

Changes in Heart Weights During Late Phase After MI

Among sham-operated animals, KO mice had larger heart weight-to-BW (HW/BW) ratios, which reflected basal myo-

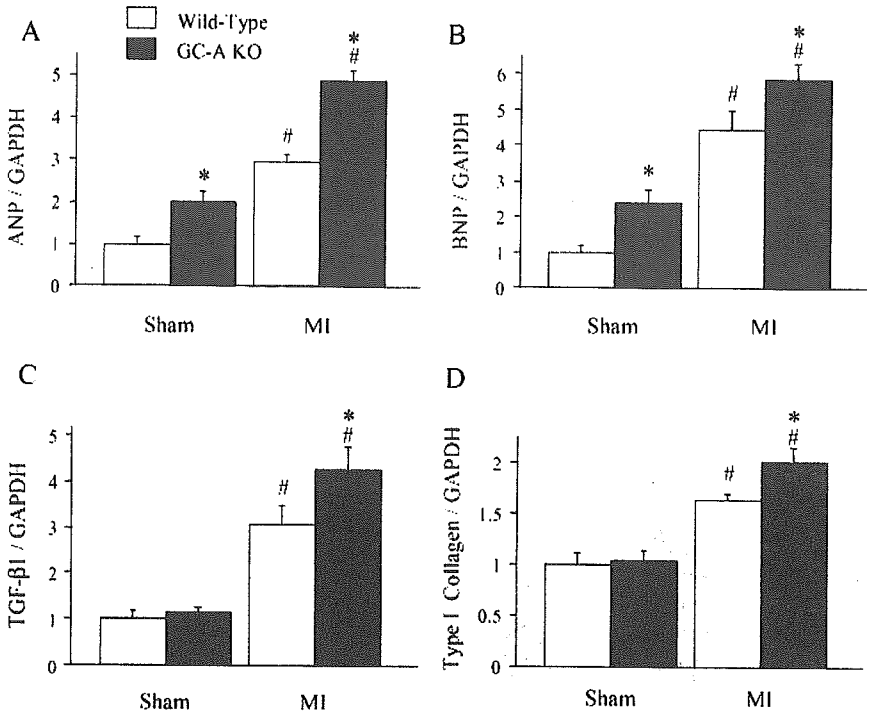

Figure 3. Relative levels of expression of ANP (A), BNP (B), TGF-β1 (C), and type I collagen (D) mRNA normalized to the corresponding GAPDH mRNA levels measured by quantitative RT-PCR in sham-operated and infarcted hearts 3 days after surgery. Mean mRNA levels in sham-operated WT hearts were assigned a value of 1.0. Values are means±SEM (n=7 to 10); *P<0.05 vs WT mice for each operation; #P<0.05 vs sham in each strain.

cardial hypertrophy (WT 5.44±0.14 mg/g versus KO 7.94±0.20 mg/g; P<0.001). Four weeks after MI, the HW/BW ratios were higher than in sham-operated mice, irrespective of genotype, but the effect was more pronounced in KO (Sham 7.94±0.20 mg/g versus MI 10.12±0.20 mg/g; 27% increase; P<0.0001) than WT (Sham 5.44±0.14 mg/g versus MI 6.29±0.14 mg/g; 16% increase; P<0.005) mice.

Myocardial Fibrosis During Late Phase After MI

As shown in Figure 4A, sections of ventricle from sham-operated KO mice showed significantly (P<0.01) more myocardial collagen accumulation than those from WT mice. Four weeks after MI, the collagen volume fraction in the noninfarcted septa was significantly increased in KO mice (P<0.0001) but not in WT mice (P=0.6). This marked difference in the degree of interstitial fibrosis in the noninfarcted septa from KO and WT mice can be seen in Figure 4B.

TABLE 2. Baseline, Week 4, and Absolute Changes From Baseline to Week 4 After MI in Echocardiographic Measurements

	WT (n=13)		GC-A KO (n=11)	
Parameters	Baseline	Week 4	Baseline	Week 4
Measurements				
LVEDD (mm)	4.55±0.08	5.76±0.08	5.11±0.10*	6.26±0.14*
LVESD (mm)	3.31±0.06	4.54±0.09	3.69±0.09*	5.28±0.12*
PWth (mm)	0.63±0.02	0.65±0.03	0.85±0.05*	1.02±0.04*
%FS (%)	27.4±0.3	21.5±1.0	27.5±0.6	15.6±0.9*
Absolute change from baseline to week 4 after MI				
Δ LVEDD (mm)	1.22±0.06		1.16±0.08	
Δ LVESD (mm)	1.24±0.09		1.59±0.09*	
Δ PWth (mm)	0.02±0.03		0.17±0.05*	
Δ %FS (%)	−5.9±1.1		−11.9±1.1*	

PWth indicates PW thickness.
Values are mean±SEM; *P<0.05 vs WT mice.

Effects of Genetic Disruption of AT1a Receptors in KO Mice

In an additional experiment, we induced MI in 8- to 10-week-old male DKO mice lacking GC-A and AT1a receptors. Although basal systolic blood pressures were significantly lower in DKO than KO mice (DKO 105.8±2.6 mm Hg; P<0.0001 versus KO mice), the high early mortality rate seen in the latter was not significantly improved in the former (Figure 5); and, as in KO mice, most of the deaths were attributable to acute heart failure (68.2%). Four weeks after MI, HW/BW ratios in DKO mice were 26% higher than in sham-operated animals (Sham 7.06±0.20 mg/g versus MI 8.88±0.42 mg/g; P<0.001), which is also similar to the response seen in KO mice. In contrast, there was no significant difference in the collagen volume fraction in the noninfarcted septa from infarcted and sham-operated DKO hearts (Figure 4A); indeed, the marked interstitial fibrosis seen in the noninfarcted septa from KO hearts was virtually absent in DKO hearts (Figure 4B).

Effects of Hydralazine Administration in KO Mice

To evaluate the involvement of blood pressure difference between WT and KO mice, we orally administered hydralazine to KO mice from 1 week before MI until 4 weeks after MI. Although systolic blood pressure was significantly reduced in hydralazine-treated KO mice (103.6±1.2 mm Hg; P<0.0001 versus nontreated KO mice), the high early mortality rate was not significantly improved (Figure 5), and histological analysis showed there to be no significant attenuation of the interstitial fibrosis in the noninfarcted septum 4 weeks after MI (Figure 4).